SHH SIGNALING IN LIMB DEVELOPMENT

By

Jiang Liu

Dissertation

Submitted to the Faculty of the

Graduate School of Vanderbilt University

in partial fulfillment of the requirements

for the degree of

DOCTOR OF PHILOSOPHY

In

Cell and Developmental Biology

May, 2013

Nashville, Tennessee

Approved:

Professor Chin Chiang

Professor Steve K. Hanks

Professor David M. Bader

Professor Anna L. Means

Professor Ethan Lee

To my family and friends

ACKNOWLEGEMENT

I would like to express my deep appreciation and gratitude to my advisor, Dr. Chin Chiang, for the patient guidance and mentorship he had granted me. I would also like to thank Dr. Ying Litingtung, a Staff Scientist in the lab and Chin's wife. Together, they have helped me with every aspect of my research and provided me with valuable opportunities to explore the beauty of science during my Ph.D study. I learned not only skills and experience, but also scientific attitudes and the way of thinking and planning about research and career. I will keep everything they have given me in my heart and carry that on to my future career.

I would also like to thank my committee members, Dr. Steve Hanks, Dr. David Bader, Dr. Anna Means, Dr. Ethan Lee, four distinguished scientists for the thought-provoking suggestions and generous help all the way along both for my thesis research and for my future career. I benefited so much from their extensive knowledge and experience, as well as their compliments and encouragements about my work over the years, which granted me the momentum to complete my thesis study. Hereby, I would like to express heartfelt thank you to each of my committee members.

I also want to acknowledge our past and present Chiang lab members for their suggestions throughout my study. One in particular is Xi Huang, a former graduate student. Xi is one of my lifetime friends and teachers, who provides me with valuable experience and collaboration since I joined the lab. Xi still kept track of my research and offered thoughtful comments about my manuscript even after he started his postdoctoral

career in UCSF. I'd like to say thank you to Xi for all those quality time he has created, and good luck for his future career.

I thank Qiang Li and Steven A. Vokes at The Institute for Cellular and Molecular Biology, University of Texas at Austin for collaborating on this project. Their ChIP findings and valuable advice are thoroughly appreciated. I thank Michael R. Kuehn at The Laboratory of Protein Dynamics and Signaling, The National Cancer Institute for providing the *Hoxb6Cre* mouse line. The hypoxia marker EF5 was made available by the NCI and obtained through Cameron Koch at the University of Pennsylvania; we thank them for this valuable reagent. The Vanderbilt Transgenic Mouse/Embryonic Stem Cell Shared Resource helped with the injection of targeted ES cells.

Finally, I would be remiss if did not acknowledge the innumerable sacrifices and unconditional supports made by my parents and my wife, Yinzi, while I pursued the PhD degree. Without them, my thesis research would never be completed. Also, my thanks to all the friends both in the CDB department and outside, who have made my life as a graduate student so enjoyable and memorable.

.

TABLE OF CONTENTS

LIST OF FIGURES

CHAPTER 1

GENERAL INTRODUCTION

Part I: Hh signaling

Tight control of cell-cell communication and cell-matrix communication are essential for embryonic patterning and development of many different organs in both invertebrates and vertebrates. The Hedgehog (Hh) family of secreted morphogenetic proteins is a critical mediator of key signaling events during embryogenesis. Malfunction of Hh signaling is associated with a variety of human developmental disorders such as holoprosencephaly, polydactyly, and tumorigenesis (Hill et al., 2003; Ingham, 1998a; Roessler et al., 1996; Taipale and Beachy, 2001). Hh was initially discovered by Christiane Nüsslein-Volhard and Eric Wieschaus nearly 30 years ago in *Drosophila* (Nusslein-Volhard and Wieschaus, 1980). The *Hh* gene is a "segment-polarity" gene that controls *Drosophila* embryonic cuticle pattern and loss of *Hh* in *Drosophila* generates a short and "spiked" phenotype of the cuticle that is reminiscent of the hedgehog.

In vertebrates, there are three members of *Hh* gene family: *Sonic hedgehog (Shh), Desert hedgehog (Dhh)* and *Indian hedgehog (Ihh)*, each with distinct expression pattern throughout embryonic development. *Shh*, the most studied member, is expressed predominantly in epithelial tissues and the nervous system. It regulates growth and patterning of specific tissues in a context-dependent manner. *Ihh* is a master regulator in bone development and a vasculogenesis regulator in the primitive endoderm. *Dhh*, which

has the closest sequence similarity to the *Drosophila Hh*, is essential for peripheral nerve system development and spermatogenesis. All Hh ligands are synthesized as a ~45kD precursor which undergoes cleavage and modification processing events resulting in a 19kD active N-ternimal fragment with a cholesterol moiety attached to its C-terminal and a palmitate modification as its N-terminal. Both cleavage and modification are critical for proper signaling activity and ligand distribution (Lee et al., 1994; Porter et al., 1996a; Porter et al., 1995; Porter et al., 1996b). As a morphogen, the Hh proteins act not only upon immediate neighboring cells to induce juxtacrine signaling but also over a long distance of ten or more cell-diameters to induce paracrine signaling. The twelve-pass transmembrane protein Dispatched (Disp) appears to be required for the release of lipidated Hh from its source for paracrine signaling (Fig. 1.1). In the absence of Disp, Hh accumulated in producing cells, hence restricted long distance distribution of Hh protein (Burke et al., 1999; Caspary et al., 2002; Kawakami et al., 2002; Ma et al., 2002). However, the detailed mechanism of how Disp facilitates Hh secretion and paracrine signaling remains largely unknown.

The Hh signaling pathway is highly conserved in both invertebrate and vertebrates. In the canonical model of Hh signal transduction, the secreted Hh ligand interacts with a 12-pass transmembrane receptor Patched (Ptc) within a receptor complex, relieving Ptc-mediated inhibition on a 7-pass transmembrane receptor Smoothened (Smo) on the surface of responding cells (Fig. 1.1). Smo then transduces the Hh signal to Gli transcription factors (Cubitus interruptus, Ci in *Drosophila*), by preventing the processing mediated inhibition on a 7-pass transmembrane receptor Smoothened (Smo) on the

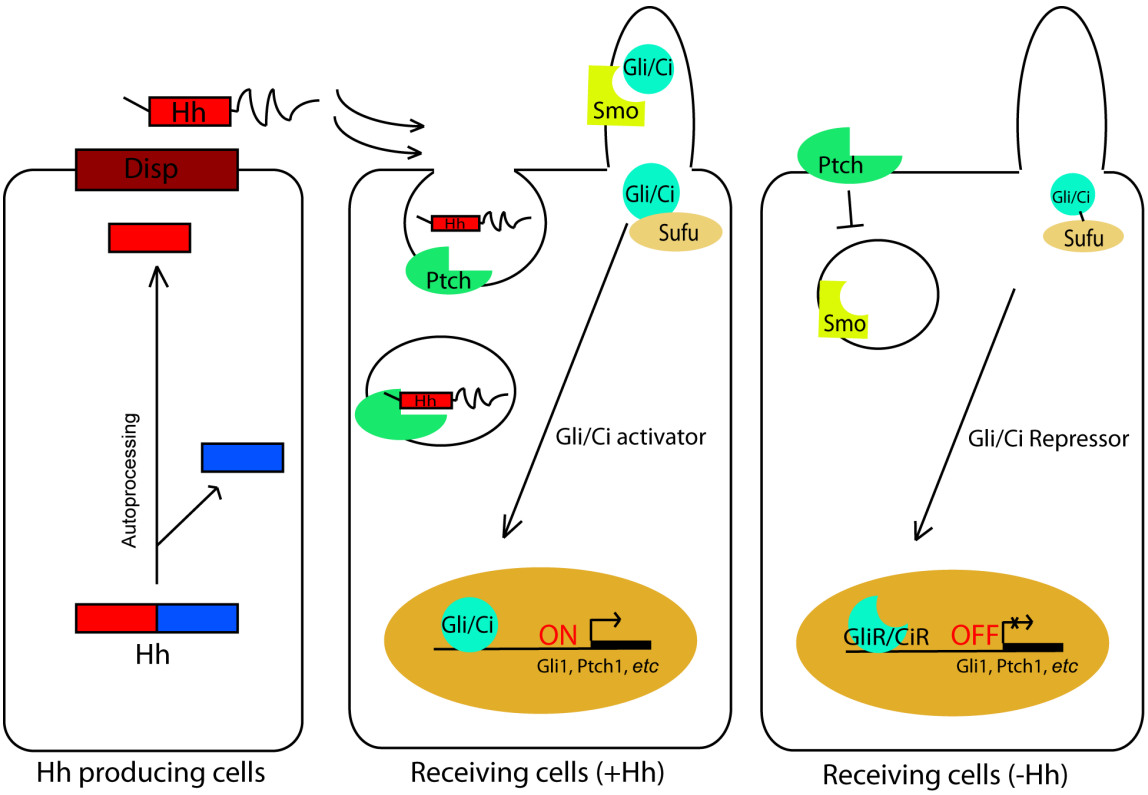
Hh
Disp
Autoprocessing
Hh
Hh producing cells
Gli/Ci
Smo
Gli/Ci
Sufu
Hh
Ptch
Hh
Gli/Ci activator
Gli/Ci
ON
Gli1, Ptch1, etc
Receiving cells (+Hh)
Ptch
Gli/Ci
Sufu
Smo
Gli/Ci Repressor
GliR/CiR
OFF
Gli1, Ptch1, etc
Receiving cells (-Hh)

Figure 1.1. A simplified Hh signaling pathway.

Modified from http://flipper.diff.org/app/pathways/info/2952

In Hh producing cells, the Hh precursor undergoes multiple processing steps including an autoproteolysis step to release its N-terminal fragment, addition of palmitate moiety to the N terminus and cholesterol moiety to the C terminus. The secretion of mature Hh from the producing cells requires the activity of the 12-transmembrane protein, Dispatch (Disp). In the range of Hh signaling, Hh protein binds to its 12-transmembrane receptor Patched (Ptch), clearing Ptch from the cell surface via endocytosis. Binding of Hh to Patched alleviates repression of a 7-transmembrane protein Smoothened (Smo), allowing the activation of Gli transcriptional factor in primary cilium, or Ci in *Drosophila*. Activated Gli or Ci will translocate into nucleus to activate Hh target genes, such as *Gli1*, *Ptch*, *etc*. In the absence of Hh, Ptch inhibits Smo and prevents its translocation to the cell surface or to the primary cilium. Without Smo activation, Gli or Ci will proceeded into its repressor form and inhibit its target genes in nucleus. Suppressor of Fused (Sufu) prevents Gli/Ci nuclear translocation and activation but also stabilizes full length Gli/Ci in cytosol.

surface of responding cells (Fig. 1.1). Smo then transduces the Hh signal to Gli transcription factors (Cubitus interruptus, Ci in *Drosophila*), by preventing the processing of full-length Glis into transcriptional repressors. Activated full-length Gli activators allow the transcription of Hh target genes in the nucleus while Gli repressors inhibit their expressions (Fig. 1.1).

In vertebrates, two Ptc isoforms, Ptch1 and Ptch2, can bind Hh proteins and interact with Smo. Ptch1 is the functional ortholog of *Drosophila* Ptc. It can bind to multiple Hh members and is widely expressed throughout the embryo. Intriguingly, Ptch1 itself is a direct target of Hh signaling, providing a negative feedback to allow receiving cells to accurately sense the morphogenic gradient and interpret a wide range of Hh concentrations. Loss of Ptch1 results in complete activation of Hh signaling and embryonic lethality (Goodrich et al., 1997). Ptch2, on the other hand, is more restricted to epidermal tissues and spermatocytes and mice with loss of Ptch2 are viable but develop skin lesions and epidermal hyperplasia (Nieuwenhuis et al., 2006).

The Gli transcription factors, or *Drosophila* Ci, are the major effectors of the Hh signaling cascade. These proteins contain five conserved zinc finger domains and a C-terminal transactivation domain. When the signal is off, the 155kD Ci protein is phosphorylated and proteolytically processed into a truncated N-terminal repressor fragment (CiR), which lack the transactivation domain and inhibits Hh target gene transcription. Presence of Hh ligand activates Smo activity and blocks Ci phosphorylation and proteolytic processing, resulting in a full-length Ci activator form that activates Hh

target genes. In vertebrates, three Gli transcription factor family members mediate the response to Hh signaling. Gli1 functions solely as a transcriptional activator whereas Gli2 and Gli3 possess both activator and repressor activities that are regulated by Hh signaling. Genetic studies indicated that Gli1 expression is dependent on Gli2 and Gli3 activator activities (Bai et al., 2004; Motoyama et al., 2003). In contrast, Gli3, and to a limited extent Gli2, are constitutively cleaved into truncated repressor forms while Hh signaling counters this process and converts them to labile activators (Litingtung et al., 2002; Pan et al., 2006; Wang et al., 2000). Mutations in vertebrate Gli genes result in various phenotypes. For instance, *Gli1* mutants as well as *Gli1/Gli2* double mutants have severe defects in the diencephalic region of the brain (Park et al., 2000). *Gli2* or *Gli2/Gli3* mutants exhibit different skeletal abnormalities (Mo et al., 1997). Mutant mice lacking *Gli2/Gli3* or *Gli1/Gli2* display strong foregut and lung defects (Motoyama et al., 1998; Park et al., 2000). However, in the limb, the effects of Shh may be exclusively mediated by Gli3. *Gli1/Gli2* double mutants display normal digit number and pattern, whereas loss of Gli3 leads to dramatic polydactyly phenotype with defective digit pattern and identity, resembling that of *Shh;Gli3* or *Gli2;Gli3* double mutants when both repressor and activator activities are abrogated (Bowers et al., 2012; Litingtung et al., 2002; te Welscher et al., 2002), indicating Gli3-mediated repression is the major regulator of digit patterns. In agreement, the gradient of Gli3 processing across the limb bud is observed in both chicken and mouse limb buds (Wang et al., 2000). While these observations underscore the importance of Gli activities in the control of Shh signaling and limb development, much less is known about downstream targets that mediate their functions.

Part II: Limb development

The vertebrate limb is a complex organ with asymmetrical skeletal elements. The number and position of each element in the forelimbs and hindlimbs are precisely organized. From proximal to distal, the limb bones consist of the stylopod (humerus in forelimb, femur in the hindlimb), zeugopod (radius and ulna in forelimb, tibia and fibula in hindlimb) and autopod (carpals in forelimb, tarsals in hindlimb). Initially, these fragments are cartilaginous which are eventually replaced by bone.

During embryogenesis, the limb bud is initiated from an outgrowth of the embryonic body wall, consisting of mesenchyme derived from the lateral plate mesoderm (LPM) and epithelium overlying the surface ectoderm. Their position is conserved throughout tetrapod, and appears to be determined by retinoic-acid-activated *Hox* gene levels along the anterior-posterior body axis. Exposing amputated tail of marbled balloon frogs to ectopic retinoic acid during regeneration resulted in a transformation of tail tissue to the limb field (Mohanty-Hejmadi et al., 1992). As limb development proceeds, mesenchyme cells from the somatic layer of the limb field LPM proliferate to create a bulge and form the initial bud (Crossley et al., 1996). The proliferation process is mainly mediated by fibroblast growth factor (Fgf) signals, such as Fgf8. Although Fgf signal induces both forelimb and hindlimb formation, their patterns are different and distinct. It is not yet known what molecular mechanism directs forelimb versus hindlimb specificity. Recent studies have shown that some transcription factors are differently expressed in the hindlimb and forelimb buds. In chick, *Hoxc-4* and *Hoxc-5* are only expressed in the wing

buds, while *Hoxc-9*, *Hoxc-10*, and *Hoxc-11* are exclusively expressed in the leg buds (Nelson et al., 1996). Similar differences are also observed in members of the transcription factors family related to *Brachyury*-like genes (*T-box* genes) in mouse. *Tbx-5* is expressed only in the mouse forelimb, while *Tbx-4* expression is only observed in the mouse hindlimb (Gibson-Brown et al., 1996). In addition, the loss of human TBX5 results in abnormalities of the heart and upper limbs, but not legs, indicating that TBX5 is only required for forelimb formation (Basson et al., 1997; Li et al., 1997).

During limb development, three orthogonal axes are generated: the dorsal-ventral (D-V) patterning axis to form limb sidedness (knuckle-side versus palm), proximal-distal patterning axis (P-D) to form limb segments, and anterior-posterior (A-P) patterning axis to generate correct digit number and identity in the autopod and radius/ulna, tibia/fibula position in the zeugopod. During the past decade, specific proteins and signaling centers that play significant roles in the formation of each of these limb axes have been identified. The D-V axis is regulated, at least in part, by Wnt7a secreted from the dorsal ectoderm (Riddle et al., 1995; Vogel et al., 1995). The P-D axis appears to be regulated by the FGF family of proteins generated at the distal tip of the emerging limb bud, known as the apical ectoderm ridge (AER) (Dudley et al., 2002; Sun et al., 2002). The A-P axis is regulated by Shh produced by a group of specialized mesodermal cells located at the posterior margin of the limb bud, known as the zone of polarizing activity (ZPA). Grafting of ZPA cells to the anterior mesoderm results in a complete mirror-image duplication of digits in chick embryos (Fig. 1.2). This phenomenon can also be mimicked by implanting Shh-soaked beads to the anterior

mesoderm, indicating that Shh protein mediates ZPA activity in the limb (Fig. 1.2) (Chang et al., 1994; Lopez-Martinez et al., 1995; Riddle et al., 1993). Moreover, the severity of limb phenotype correlates with the concentration of Shh protein. Beads soaked in high Shh concentration induce more posterior digits than low-concentration Shh beads, suggesting that Shh signaling progressively specifies digits with posterior identities through dose-dependent activation of putative Shh effectors (Yang et al., 1997). Accordingly, mouse *Shh-/-* mutant embryos lack the ZPA, show truncated skeletal elements and lose all digits except digit 1 in the hindlimb, suggesting that Shh is not required to specify digit 1 identity (Chiang et al., 2001; Chiang et al., 1996; Kraus et al., 2001; Lewis et al., 2001). The above central signals often interact with each other during limb development. For example, Shh signaling in the ZPA is positively regulated by Fgf signals from the AER (Niswander et al., 1994; Riddle et al., 1993). This positive loop stabilizes *Fgf* expression, permitting proliferation and survival of mesenchymal precursors, resulting in reduction of Shh signal as the limb grows beyond the influence of Fgf from the distal end (Towers et al.; Zhu et al., 2008).

Retinoic acid (RA) has long been known to induce ZPA activity in the limb. Beads soaked in RA can induce an ectopic Shh expression in anterior limb and induce a mirror-image reversal of A-P polarity. However, RA is not sufficient to induce complete ectopic posterior digit formation but rather induces a cofactor of Shh. The induction of most 5' *HoxD* genes by Shh could be achieved only if RA is present (Ogura et al., 1996). Recent studies have suggested that activation of Shh target genes specifically in the posterior limb bud, but not the anterior, is determined by Hand2 and a long-range Shh enhancer

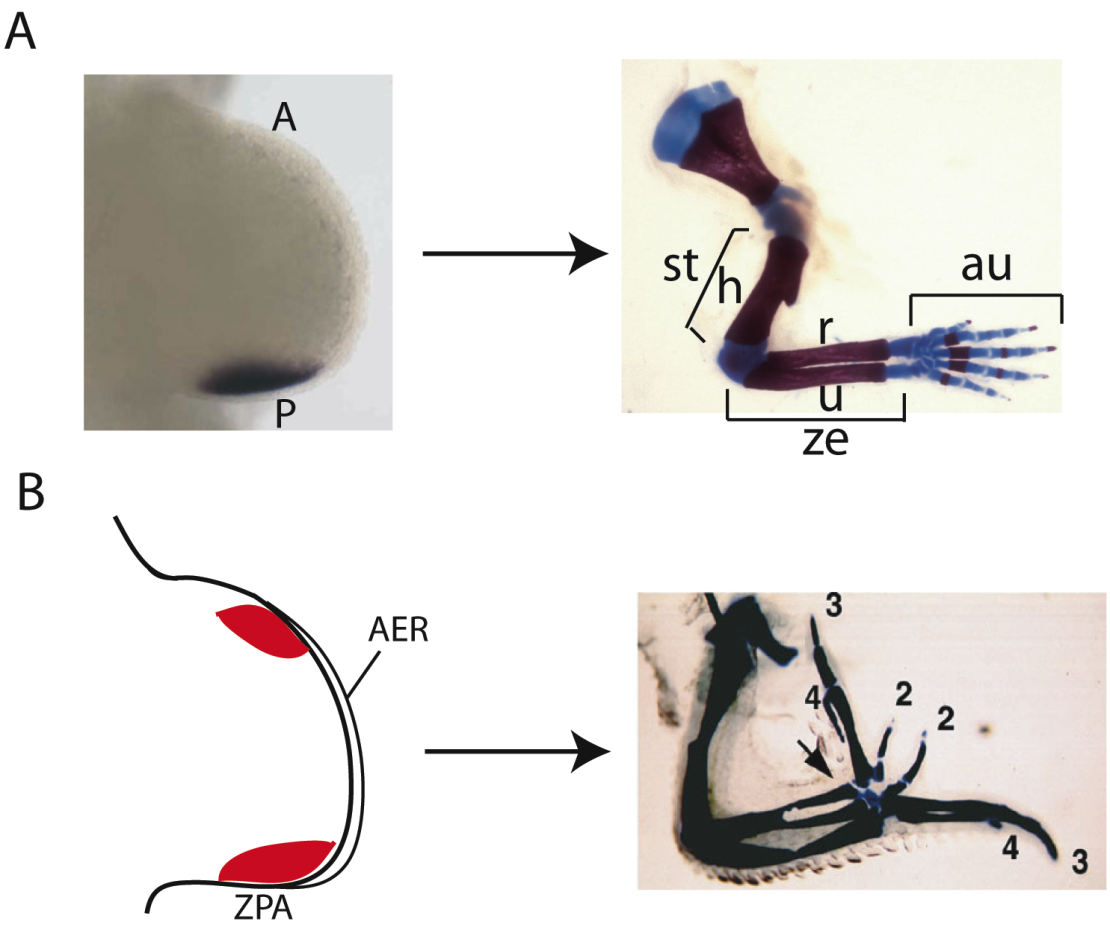

Figure 1.2. Shh mediates the zone of polarizing activity (ZPA) in the limb.

A, the limb bud develops into three segments: the stylopodium (st), zeugopodium (ze) and autopodium (au). Note *Shh* expression in the posterior ZPA. **B**, Grafting of the ZPA or Shh-soaked beads to the anterior margin of the limb mesoderm (red) induces a mirror-image duplication of digits in chick (Riddle et al., 1993). Note that arrow in B highlights the duplicated radius (r). Abbreviations: h, humerus; u, ulna

named ZPA regulatory sequence (ZRS). *Hand2* encodes a basic helix-loop-helix transcription factor that is expressed earlier than *Shh* in the posterior limb mesoderm but its expression in the anterior domain is repressed by Gli3. Inactivation of *Hand2* disrupts posterior limb identity and *Shh* expression, which resulted in a similar digit phenotype as *Shh* null mutant (Liu et al., 2009). Biochemistry studies also revealed that Hand2 interacts with Hoxd13(Galli et al., 2010), another essential Shh regulator, as well as other cofactors such as E12 and Twist1 (Dai and Cserjesi, 2002; Firulli et al., 2005; Markus and Benezra, 1999; Zuniga et al., 2002). ZRS is an evolutionarily conserved *cis*-regulatory region located about 800 Kb upstream of the *Shh* gene (Lettice et al., 2003). Mice carrying mutation in core ZRS sequence displayed limb bud-specific loss of *Shh* expression and recapitulate the limb skeletal phenotype of *Shh* null mutants (Sagai et al., 2005). Point mutation in human ZRS sequences also causes congenital preaxial polydactylies (PPD), with abnormality in skeletal patterning (Hill, 2007).

How Shh signaling specifies the A-P axis is still not fully deciphered. The classic morphogen gradient model suggests that tissues respond differently to different concentrations of Shh secreted by the ZPA at the posterior margin, whereas the most posterior digit receives the highest cumulative Shh level. Yet, later works indicate that the most posterior Shh-expressing cells only transiently respond to Shh but become refractory to Shh signals over time (Ahn and Joyner, 2004; Marigo et al., 1996; Platt et al., 1997). These observations led to a temporal gradient model in which Shh signaling is only temporally required for early specification. More recent study suggests that the completion of digit patterns combines an early pre-specification stage and a later

precursor expansion stage. Shh is not only required early in pre-patterning, but also needed in the expansion stage to ensure adequate cell survival and proliferation (Zhu et al., 2008). Although a number of studies have suggested cell expansion and migration in limb development, however, not much migration has been observed. It is also possible that the expansion of precursors at later stages is dependent on long-distance Shh paracrine signaling. By tracing descendants of Shh- expressing cells, studies have shown that Shh-expressing cells contribute to digits 4, 5 and the posterior half of digit 3. Similar fate mapping studies, by tracing descendants of Shh-responsive cells, have concluded that digits 2-5 are derived from precursors that have received the Shh signal. These observations suggest that at least digit 2 relies on paracrine Shh signaling or is derived from early Shh-responsive cells. However, additional studies are required to clearly address the requirement of paracrine Shh signaling in limb development. Another major gap that remains to be fulfilled is to identify the downstream targets of Shh signaling during limb development. Recent genome-wide chromatin immunoprecipitation (ChIP) studies using mouse limb buds derived from transgene expressing an epitope-tagged Gli3 have identified over two hundred putative direct Gli target genes, highlighting the complexity of the regulatory landscape (Vokes et al., 2008).

Part III: Early chondrogenesis and joint patterning

As I have discussed in the last chapter, Shh regulates A-P patterning of the developing limb bud, focusing mainly on skeletal patterning. However, more recent evidence indicates Shh not only pre-patterns digit numbers and identity, but also regulates the proliferation and growth of limb mesenchyme cells (Lopez-Rios et al., 2012; Zhu et al.,

2008). Some studies have suggested that Shh can also promote chondrogenesis in conjunction with bone morphogenetic protein (Bmp) signaling in micromass culture experiments (Murtaugh et al., 1999). In addition, ectopic Shh expression in chondrocyte lineage cells results in fusion of skeletal elements and abnormal joint formation (Tavella et al., 2006). Thus, whether and how Shh signaling affects early chondrogenesis and joint patterning in limb development remain to be determined.

Chondrogenesis is the early phase of cartilage formation, including mesenchyme proliferation, precartilagenous condensation and chondrocyte differentiation. The mesenchyme cells closest to the AER receive Fgf4, Fgf8 secreted from the AER. This region of proliferation is called the progress zone. Fgf10 is thought to be the major proliferative signal expressed in the progress zone to maintain cell division. As the limb bud grows, the cells leave the progress zone and differentiate in a regionally specific manner. Early leaving cells form proximal structure such as the stylopod, those cells that undergo more divisions leave the progress zone later and form more distal structure such as the autopod. This model is supported by AER removal experiment in chick. When AER is ablated from an early-stage wing bud, only the humerus forms. When the AER is removed slightly later, humerus, radius, and ulna form (Rowe et al., 1982).

Mesenchyme cells leaving the progress zone begin to express extracellular matrix proteins that cause them to undergo condensation into nodules (Hall and Miyake, 1995). Prior to condensation, the extracellular matrix surrounding precartilage mesenchymal cells is rich in hyaluronan and collagen type I (Fig. 1.3). Hyaluronan deposition is

dramatically reduced when condensation begins (Fig. 1.3) (Knudson and Toole, 1985; Kosher and Savage, 1981; Kulyk and Kosher, 1987), probably due to less synthesis as well as increased degradation by hyaluronidase. A lower hyaluronan environment allows cell-cell interaction to occur. Meanwhile, the condensing cells begin to express cell adhesion molecules, neural cadherin (N-cadherin) and neural cell adhesion molecule (Fig. 1.3) (N-CAM) (Hall and Miyake, 1995; Oberlender and Tuan, 1994). Once condensed, the cells become chondrocytes and begin secreting chondrocyte-specific extracellular proteoglycans and collagens. N-cadherin and N-CAM disappear and are only detectable in perichondrial cells. Transforming growth factor beta (Tgf-β) has been suggested to play a critical role in initiating chondrogenic condensation. It induces fibronectin synthesis, which regulate N-CAM, and participate in setting the condensation boundary with another N-CAM negative regulator syndecan (Eames et al., 2003; Olsen et al., 2000).

Soon after condensation, the central cartilaginous cells become dramatically larger and deposit cartilage matrix containing collagen II, IX, and XI and aggrecan, the major cartilage proteoglycan. These cells residing in the cartilage anlagen become hypertrophic chondrocytes, while the cells surrounding the central nodule cells differentiate to form the periosteum. Sox9, a member of the HMG-box DNA-binding transcription factor, is one of the earliest markers expressed in condensing cells. It is required for the expression of the type II collagen (Col2a1), as well as other cartilage-specific matrix proteins such as Col11a2 and CD-RAP (Eames et al., 2003; Lefebvre et al., 1998; Ng et al., 1997). Bmp signaling appears to be critical for Sox9 expression (Yoon et al., 2005). Bmp signaling is transduced through the formation of heteromeric complexes of type I and II receptors,

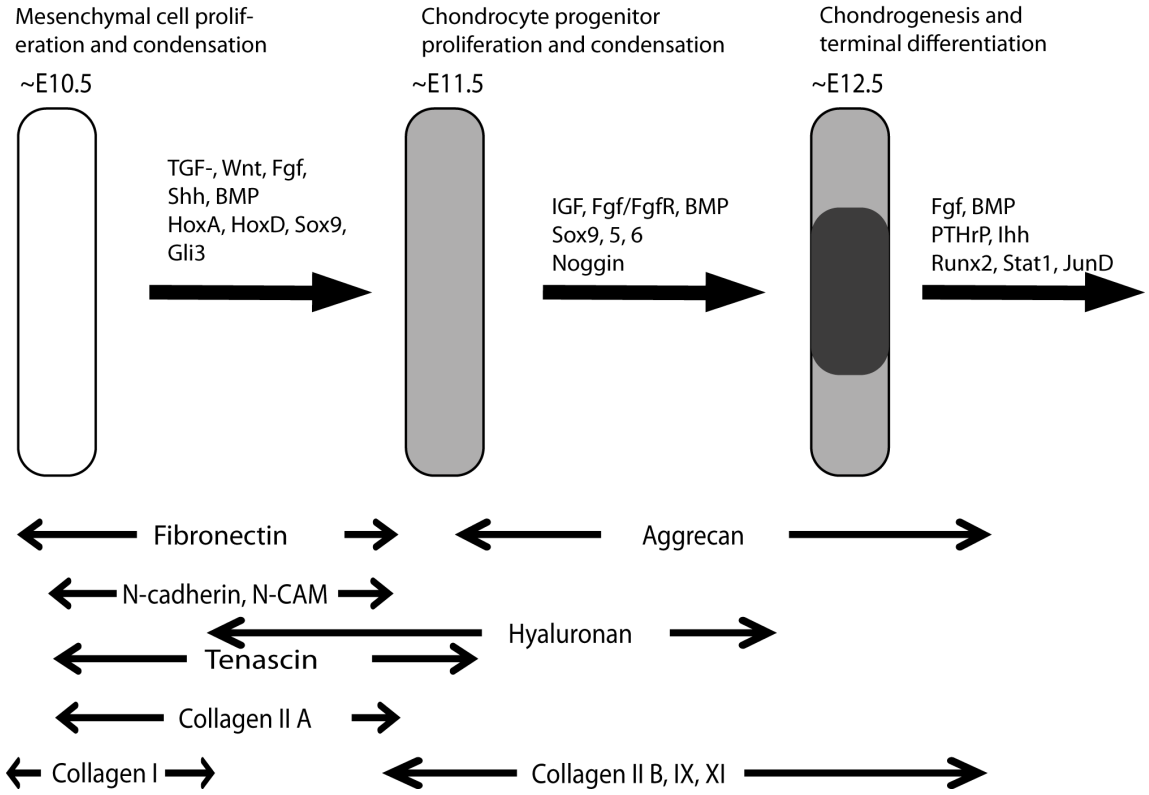

Figure 1.3. Sequence of events of early chondrogenesis during the development of bones.

Modified from Goldring et al., *J Cellular Biochemistry*, 2007 (Goldring et al., 2006)

The different stages of mouse chondrogenesis are distinguished by the temporal patterns of extracellular matrix components indicated below or expression patterns of signaling molecules and transcriptional factors indicated above the arrows. See texts for more detail.

BmpR1A and BmpR1B in chondrocyte condensation. Upon ligand binding, the type II receptor phosphorylates the type I receptor, which is also a serine-threonine kinase that can phosphorylate Smad proteins. Canonical Bmp signal involves Smads1, 5, and 8. They form a complex with Smad4 upon Bmp induction, which then translocates to the nucleus to promote transcription of target genes. Bmps can also signal through Tgf-β activated kinase 1 (TAK1), which can activate p38 and JNK cascades, or activate Ras/Erk1/2 signaling to regulate chondrogenesis in a positive manner(Nakamura et al., 1999; Seghatoleslami et al., 2003).

During the process of chondrocyte hypertrophy, blood vessel cells from the surrounding periosteum invade the center of the hypertrophic cartilage. As the cartilage matrix is degraded, hypertrophic cartilage cells die, and osteoblasts from blood vessels begin to secrete bone matrix to replace the cartilage matrix. Eventually, all the cartilage is replaced by bone.

The synovial joint sits between two or more skeletal elements. It consists of articular cartilage, bone, ligament, synovium and fibrous capsule. Joints are also target sites of diseases, the most common being osteoarthritis and rheumatoid arthritis. However, little is known about how they develop. In condensing cartilage, a group of cells lose their rounded shapes and become flattened to specify a nonchondrogenic region termed the joint interzone (Fig. 1.4 Step 1). As the interzone develops, this region can be resolved into three layers; a thin central layer of elongated cells between two closely compacted articular surface layers on each side (Fig. 1.4 Step 2). The middle layer is thought to

undergo apoptosis and enzymatic degradation of the interzone to form the joint cavity (Andersen, 1961; Merida-Velasco et al., 1997). The articular surface layers specify articular cartilage and tissues surrounding the joint (Fig. 1.4 Step 3).

Although the mechanism of interzone formation remains to be elucidated, recent studies have suggested that Wnt14 is selectively expressed in the interzone. Forced retroviral-mediated Wnt14 expression in chick limb resulted in a ectopic joint structure, indicating that Wnt14 may be an early inducer of interzone formation (Hartmann and Tabin, 2001). However, overexpression of β-catenin, the downstream effector of Wnt14, does not recapitulate the ectopic joint formation in chicken limb, suggesting that Wnt14 may mediate joint formation through non-canonic Wnt pathway (Hartmann and Tabin, 2000). Another well-known marker for the interzone is Growth and differentiation factor 5 (Gdf5), which belongs to the Tgf-β family. *Gdf5* expression in the interzone is first detectable at ~E12 in the perichondrium bordering the condensing digit rays (Storm and Kingsley, 1996). As development proceeds, perichondrial *Gdf5* expression diminishes while interzone expression becomes more prominent. However, the role of Gdf5 is paradoxical. Gdf5 does not specify joint formation. In fact, Gdf5 promotes chondrogenesis and chondrocyte proliferation, which inhibits noncartilaginous joint formation (Francis-West et al., 1999a; Merino et al., 1999). Surprisingly, *brachypod* mutant mice, which harbor mutant *Gdf5* allele, display appendicular skeletal defects, including absence of some joints. Similar joint defects were also observed in humans carrying mutant *GDF5* allele(Francis-West et al., 1999b). These discrepancies underscore the complexity of joint initiation, which may involve cell-cell interaction between

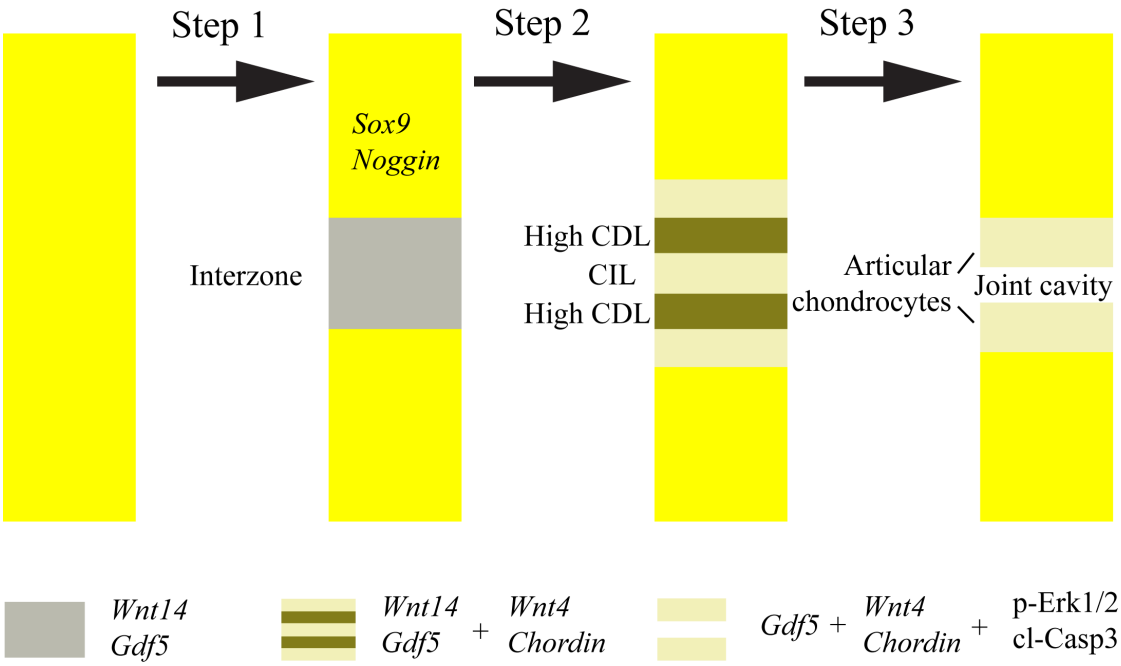

Figure 1.4. Joint development and cavity formation within developing skeletal elements

Modified from Karsenty et al. *Dev Cell 2002* (Karsenty and Wagner, 2002)

Condensing cartilage mesenchyme cells express *Sox9* and *Noggin* during chondrogenesis. However, a group of cells lose *Sox9, Noggin* expression and become flattened to specify a nonchondrogenic region termed the joint interzone, which will express *Wnt14* and followed by *Gdf5*. As the interzone develops, this region start to express *Wnt4*, *Chordin*, and can be resolved into three layers; a thin central layer of elongated cells between two closely compacted articular surface layers on each side. The middle layer is thought to undergo apoptosis and enzymatic degradation of the interzone to form the joint cavity, which can be marked by p-Erk1/2 and cleaved-Caspase 3. The articular surface layers specify articular cartilage and tissues surrounding the joint.

interzone cells and surrounding condensing chondrocytes.

Many factors have been postulated to play a role in forming the synovial cavity. These factors include apoptosis, enzymatic degradation, differential matrix synthesis and mechanical influences. The requirement of apoptosis during cavitation is still debatable. Some studies detected apoptosis within the interzone prior to cavitation(Kimura and Shiota, 1996; Mori et al., 1995); while more recent data suggest that cell death is minimal or undetectable (Kavanagh et al., 2002). Alteration of matrix content during the cavitation process is mediated by both enzymatic turnover and new component synthesis. Articular cartilage secretes matrix metalloproteinase into the cavity, which may contribute to cartilage matrix turnover (Gepstein et al., 2002). Hyaluronan, and its cell surface receptor, CD44, are expressed abundantly in the joint interzone and developing articular surface (Craig et al., 1990). Also, it has been shown that uridine diphosphoglucose dehydrogenase activity (UDPGD), an essential enzyme in the synthesis of HA, was upregulated just prior to cavitation (Edwards et al., 1994; Pitsillides et al., 1995). Increased HA synthesis is thought to facilitate tissue separation and create joint cavity. Differential HA synthesis in the joint cavity seems to be regulated by mechanical stimuli. Immobilizing joint tissue during cavitation resulted in significant reduction of hyaluronan content and fusion of adjacent elements (Osborne et al., 2002). Mechanical stimuli also promoted MEK-ERK1/2 activation in the joint cavity, another important pathway that controls HA matrix assembly (Bastow et al., 2005).

In summary, early chondrogenesis is a complex process controlled exquisitely by cell-cell communication, cell-matrix interaction, intracellular signaling factors, and transcription of specific target genes. However, gaps in our knowledge still remain in understanding the molecular mechanism by which signaling pathways regulate cell behaviors and matrix properties in a temporal-spatial manner. In particular, the role of Shh signaling in early chondrogenesis and joint patterning is largely elusive.

Part IV: Hyaluronic Acid Synthase 2

Hyaluronic acid (HA) is a major glycosaminoglycan (GAG) component of the extracellular matrix. It is a huge linear molecule composed of repeating disaccharide units of D-glucuronic acid and N-acetyl-D-glucosamine. Together with chondroitin sulfate proteoglycans (CSPGs), HA forms an aggregate network stabilized by link proteins. This supramolecular complex is thought to regulate various cell functions by promoting adhesion, migration, proliferation and signal transduction (Day and Prestwich, 2002; Lee and Spicer, 2000; Toole, 2004; Turley et al., 2002). In cartilage matrix, HA is mainly associated with aggrecan, a CSPG subtype that contains three globular domains, G1, G2, and G3, and two extended regions including a GAG attachment region. Aggrecan-link protein-HA constitutes vast aggregates that determine the biomechanical properties of cartilage. Thus, immobilizing aggrecan in cartilage is one of the most important functions of HA during skeletal development.

HA synthesis requires a class of membrane proteins called hyaluronan synthases (Has). Vertebrates have three Has isoforms, Has1, Has2, and Has3. Each isoform is uniquely

expressed, while Has2 is the most important synthase during embryogenesis. Lacking *Has1* or *Has3* genes in mice is not lethal (Tien and Spicer, 2005). In contrast, ablation of *Has2* gene resulted in embryonic lethality at E9.5 (Camenisch et al., 2000). *Has2* appears to play a key role in producing HA for cartilage matrix. Treating human chondrocytes with antisense oligonucleotides that block *Has2* translation significantly reduced HA and aggrecan deposition in the pericellular matrix (Nishida et al., 1999). HA-rich matrices are also thought to provide a highly hydrated environment to help separate mesenchymal cells from each other, preventing cell-cell or cell-matrix interactions needed for migration (Kosher et al., 1981). During limb development, *Has2* is abundantly expressed by the AER and distal subapical mesenchymal cells (Li et al., 2007b). Consistent with this, bFGF was subsequently shown to stimulate HA synthesis in cultured chick embryonic limb mesodermal cells (Munaim et al., 1991). Other *in vitro* studies also showed that *Has* expression can be regulated by growth factors and cytokines (Jiang et al., 2011). However, the signal that induces the expression of *Has* during limb development is not known.

Aims of the Dissertation

Sonic hedgehog (Shh), a secreted signaling molecule, has been established as a morphogen essential for patterning and growth of many embryonic tissues. In the developing mouse limb bud, Shh generated from the posterior limb margin, also known as the zone of polarizing activity (ZPA), is essential in regulating anterior/posterior patterning. Abnormal digit numbers and identities are often associated with perturbation of the Shh signaling pathway. Shh acts not only upon immediate neighboring cells to

induce juxtacrine signaling but also over a short distance of a few cell diameters to a long distance of 10 or more cell diameters to induce paracrine signaling during limb patterning. However, major gaps remain in our understanding of the molecular mechanisms by which Shh signaling is regulated and interpreted during limb development. My preliminary microarray analysis revealed that *Has2* could be one of the potential targets of Shh signaling in early limb development. Thus, my thesis studies are aimed at addressing (1) the regulation of Shh signaling on putative downstream effector *Has2,* (2) the roles of Shh-mediated *Has2* in early limb development, and (3) the contribution of paracrine signaling in digit pattern formation. Gaining this knowledge will advance our understanding of the multifaceted roles played by Shh signaling in limb organogenesis and other biological processes.

1. To determine if *Has2* is a bona fide target regulated by Shh signaling.

In an attempt to identify novel downstream target genes of the Shh pathway, I performed a mouse limb bud gene expression microarray screen. I found that *Hyaluronic Acid Synthase 2* (*Has2*) expression is enriched in the posterior limb bud where Shh signaling activity is prominent. At the embryonic stages, *Has2* is responsible for synthesizing hyaluronic acid (HA), a high molecular weight non-sulfated glycosaminoglycan and a main component of the extracellular matrix (ECM). To address whether *Has2* expression is regulated by *Shh* signaling, the *Has2* expressions were examined in $Shh^{-/-}$ mutants and $Gli3^{xt}$ (*Gli3* loss of function mutant) mutants in different developmental stages including E9.5, E10.5, and E11.5. Through *in silico* analysis, we identified two consensus sequences within the 3 kb *Has2* regulatory region, one at -646bp (Gli-binding site 1,

GBS1) and the other at +504bp (GBS2) from the *Has2* transcriptional start site (+1). The Gli1 responsiveness of these GBSs was analyzed in cell-based luciferase assay by generating mutations on each GBS. To determine whether Gli can directly bind to GBSs at the *Has2* promoter region *in vivo,* Chromatin immunoprecipitation (ChIP) assays were performed in *Prx1-cre; RosaGli3T*$^{Flagc/c}$ transgenic embryos in which FLAG-tagged Gli3 repressor is expressed specifically in limb buds. Gli3R binding DNA content were enriched by FLAG antibody IP and determined by q-PCR analysis.

2. To understand the roles of Shh-mediated *Has2* in limb development

To elucidate the role of Shh-induced *Has2* in early limb development, we generated a *Has2* conditional knockout allele (*Has2*^{fl}) to circumvent the early lethality of *Has2* null mutants (Camenisch et al., 2000). We selected *Hoxb6-cre* to inactivate *Has2* function in the early limb. The *Has2 conditional-knock-out (Has2cko)* mutant mice have defects in joint patterning and chondrogenesis. Histological analysis and skeleton preparation examined the morphological changes in the phalangeal joints. *In situ* hybridization analysis examined the specific joint marker expression, including *Gdf5*, *Wnt4*, *Chordin* and other non-joint lineage genes expression, such as *Sox9*, *Noggin*, *Col2a1*. Chondrogenesis defects were examined by Alcian Blue staining and *Col2a1 in situ* hybridization in micromass cultures. HA is a major glycosaminoglycan component of the extracellular matrix, and together with chondroitin sulfate proteoglycans (CSPGs), forms an aggregate network stabilized by link proteins. Moreover, the profound joint patterning defects observed in our *Has2* conditional mutants are strikingly similar to mouse mutants that are either deficient in CSPG or imbalanced in proteoglycan sulfation (Sohaskey et al.,

2008; Wilson et al., 2012). We therefore examined the expression of CSPG and link protein by immunohistochemistry. Collectively, our findings highlight a crucial role for HA in assembling the pericellular CSPG matrix for proper mesenchymal condensation and subsequent interzone positioning.

3. To define the functional roles of paracrine Shh signaling in limb patterning

Genetic studies in *Drosophila* revealed that transmembrane protein Disp is required in Hh-producing cells to release Hh for paracrine signaling in the wing imaginal disc. Thus, Hh accumulates in the compartment boundary in the absence of Disp. Disp1-deficient mouse embryos die around E9.5 before the formation of limb patterns. To circumvent early lethality, I utilized Cre-Loxp technology to generate *Disp1* conditional knockout mutants to selectively remove *Disp1* function in the limb. Skeletal preparation was performed to examine the digit phenotype in *Disp1cko* mutant. *In situ* hybridization analysis will examine the gene expression of Shh signaling targets, including *Gli1, Ptch1*, and other digit patterning markers, such as *Hoxd13, Gremlin, Fgf4,* and *Noggin.*

CHAPTER II

SONIC HEDGEHOG SIGNALING DIRECTLY TARGETS *HYALURONIC ACID SYNTHASE 2*, AN ESSENTIAL REGULATOR OF PHALANGEAL JOINT PATTERNING

Abstract

Sonic hedgehog (Shh) signal, mediated by the Gli family of transcription factors, plays an essential role in the growth and patterning of the limb. Through analysis of the early limb bud transcriptome, we identified a posteriorly-enriched gene, *Hyaluronic Acid Synthase 2* (*Has2*), which encodes a key enzyme for the synthesis of hyaluronan (HA), as a direct target of Gli transcriptional regulation during early mouse limb development. *Has2* expression in the limb bud is lost in *Shh* null and expanded anteriorly in *Gli3* mutants. We identified an ~3 kb *Has2* promoter fragment that contains two strong Gli-binding consensus sequences, and mutation of either site abrogated the ability of Gli1 to activate *Has2* promoter in a cell-based assay. Additionally, this promoter fragment is sufficient to direct expression of a reporter gene in the posterior limb mesenchyme. Chromatin immunoprecipitation of DNA-Gli3 protein complexes from limb buds indicated that Gli3 strongly binds to the *Has2* promoter region, suggesting that *Has2* is a direct transcriptional target of the Shh signaling pathway. We also showed that *Has2* conditional mutant ($Has2^{cko}$) hindlimbs display digit-specific patterning defects with longitudinally shifted phalangeal joints and impaired chondrogenesis. $Has2^{cko}$ limbs show less capacity for mesenchymal condensation with mislocalized distributions of

chondroitin sulfate proteoglycans (CSPGs), aggrecan and link protein. *Has2*^{cko} limb phenotype displays striking resemblance to mutants with defective chondroitin sulfation suggesting tight developmental control of HA on CSPG function. Together, our study identifies *Has2* as a novel downstream target of Shh signaling required for joint patterning and chondrogenesis.

Introduction

The Hedgehog family of secreted proteins control growth and patterning during embryogenesis. Sonic hedgehog (Shh) is the most studied vertebrate member and its role has been extensively investigated in the context of limb development. The vertebrate limb originates from the lateral plate mesoderm as a bud-like outgrowth of mesenchymal cells surrounded by an ectodermal layer. Shh expression in the posterior margin of the limb bud defines the zone of polarizing activity, a signaling center that regulates anterior-posterior polarity and distal outgrowth of the limb through a positive feedback interaction with fibroblast growth factor (Fgf) secreted from the apical ectodermal ridge (Niswander et al., 1994; Riddle et al., 1993). This positive loop stabilizes Shh expression, permitting proliferation and survival of mesenchymal precursors that prefigure digit numbers and pattern (Towers et al., 2011; Zhu et al., 2008). Accordingly, the global inactivation of *Shh* leads to truncations of all distal skeletal elements except for a single un-ossified digit 1 (Chiang et al., 2001).

The response to Shh signaling is mediated by three Gli transcription factor family members. Gli1 functions solely as a transcriptional activator whereas Gli2 and Gli3

possess both activator and repressor activities that are regulated by Shh signaling. Genetic studies indicated that Gli1 expression is dependent on Gli2 and Gli3 activator activities (Bai et al., 2004; Motoyama et al., 2003). In contrast, Gli3, and to a limited extent Gli2, are constitutively cleaved into truncated repressor forms while Shh signaling counters this process and converts them to labile activators (Litingtung et al., 2002; Pan et al., 2006; Wang et al., 2000). The loss of Gli3 function leads to polydactyly with defective digit pattern and identity, resembling that of *Shh;Gli3* or *Gli2;Gli3* double mutants when both repressor and activator activities are abrogated (Bowers et al., 2012; Litingtung et al., 2002; te Welscher et al., 2002). While these observations underscore the importance of Gli activities in the control of limb development, much less is known about downstream targets that mediate their functions. Recent genome-wide chromatin immunoprecipitation (ChIP) studies using mouse limb buds derived from transgene expressing an epitope-tagged Gli3 have identified over two hundred putative direct Gli target genes, highlighting the complexity of the regulatory landscape (Vokes et al., 2008).

Using genome-wide microarray analysis of dissected anterior and posterior halves of mouse limb buds, we identified *Hyaluronic acid synthase 2* (*Has2*) as a posteriorly-enriched gene. Although *Has2* is one of three members of the *Has* family, it encodes the enzyme regulating hyaluronan (HA) biosynthesis during mouse embryogenesis as *Has2* null mutants fail to produce HA and die at E9.5-10; in contrast, *Has1* and/or *Has3* null mutants do not exhibit obvious defects, are viable and fertile (Camenisch et al., 2000). HA is a major glycosaminoglycan component of the extracellular matrix, and together with chondroitin sulfate proteoglycans (CSPGs), forms an aggregate network stabilized

by link proteins. This supramolecular complex is thought to regulate various cell functions by promoting adhesion, migration, proliferation and signal transduction (Day and Prestwich, 2002; Lee and Spicer, 2000; Toole, 2004; Turley et al., 2002). Embryos in which *Has2* has been conditionally deleted from the limb bud using *Prx1-cre* display partial proximal phalangeal duplications with defective joints that lack distinct cavities (Matsumoto et al., 2009). However, null mutations that disrupt CSPG function showed earlier, more severe phalangeal patterning defects (Sohaskey et al., 2008; Wilson et al., 2012), suggesting either that the functional complex can still be retained in the absence of HA or that the less severe phenotype in *Has2* conditional knockout represents a partial loss of function.

In this study, we showed that *Has2* expression is dependent on Shh signaling and is ectopically activated in *Gli3* mutant limb buds. Furthermore, we identified two cooperative Gli-binding sites (GBS1 and GBS2) within 3 kb of the *Has2* genomic region, and mutating these sites abolished Gli1-mediated reporter activation in a cell based assay. Chromatin immunoprecipitation of mouse limb buds showed that Gli3 strongly interacts with the region encompassing both GBS1 and GBS2. We also showed that the *Hoxb6-cre* driven *Has2* conditional mutants exhibit severe patterning defects within digits where joints are shifted perpendicularly, closely resembling mutants with defective chondroitin sulfate synthesis or metabolism. Therefore, our findings place *Has2* as an important downstream effector of Shh signaling in the developing limb that is required to establish joint patterning within digits by stabilizing HA-CSPG complexes.

Materials and Methods

Gene expression profiling analysis

E10.5 limb buds from eight litters, with 12-15 embryos per litter, were collected in cold PBS and bisected into anterior and posterior halves. Total RNAs were extracted from anterior and posterior halves using Trizol and purified using RNeasy Mini kit (Qiagen, CA). Microarray analysis on ~300ug RNA from each sample was carried out by the Vanderbilt Microarray Core facility using Affymetrix Mouse Exon 1.0 ST Array. RNA samples were also reverse transcribed using iScript cDNA synthesis kit (Bio-Rad, CA) and subjected to RT-PCR using primer sets as follows: *Has2* Forward: 5'-GTCCAAGTGCCTTACTGAAACTCCC-3'; *Has2* Reverse: 5'-GAGGATGTTCCAGATTTTACCCCTG-3'; *Gli1* Forward: 5'-CTGGAGAACCTTAGGCTGGA-3'; *Gli1* Reverse: 5'-CGGCTGACTGTGTAAGCAGA-3'; *Shh* Forward: 5'-TCTGTGATGAACCAGTGGCC-3'; *Shh* Reverse: 5'-GCCACGGAGTTCTCTGCTTT-3' and *Gapdh* Forward: 5'-TTCACCACCATGGAGAAGGC-3'; *Gapdh* Reverse: 5'-GGCATGGACTGTGGTCATGA-3'.

Animals

The *Has2* conditional targeting construct was generated using the recombineering technique as previously described (Copeland et al., 2001; Liu et al., 2003). Briefly, a genomic region of 9.5 kb, spanning exon 2 of *Has2*, was retrieved from a BAC clone (ID: bMQ-150M3) into a diphthera toxin (DTA)-expressing plasmid by recombineering. A loxp site was then inserted 50 bp upstream of exon 2, followed by the integration of frt-

neo-frt-loxp cassette 500 bp downstream of exon 2 via two rounds of recombineering. The resulting *Has2* targeting vector contained 5' and 3' homologous arms, two loxp sequences flanking exon 2, a flp recombinase removable neo cassette and the DTA gene (Fig. 2.1). To generate *Has2* conditional knockout allele, the NotI-linearized targeting vector was electroporated into mouse R1 ES cells (Nagy et al., 1993). Colonies that were negative for DTA and resistant to G418 selection were further screened by Southern blotting after HindIII digestion and analyzed by PCR to identify correctly targeted ES clones (Fig. 2.1). Targeted ES cells were injected into C57Bl6 blastocysts through the Vanderbilt Transgenic Mouse/Embryonic Stem Cell Shared Resource, and strong chimeras were subsequently backcrossed with Black Swiss mice to obtain germline transmission mice that carried heterozygous *Has2* targeted allele. The *neo* selection cassette was then removed by crossing the heterozygous mice with *flpe* mice expressing flp recombinase (Rodriguez et al., 2000) to generate $Has2^{flox}$ mice. Limb specific deletion of *Has2* was achieved by crossing to the *HoxB6*-cre line (Lowe et al., 2000). $Shh^{-/-}$ and $Gli3^{xt}$ mice were as previously described (Litingtung et al., 2002).

In situ hybridization and immunohistochemistry

Whole mount and section in situ hybridizations were performed using digoxygenin-labeled riboprobes as previously described (Li et al., 2008; Li et al., 2006). Riboprobes were synthesized using the digoxygenin RNA labeling kit (Roche).

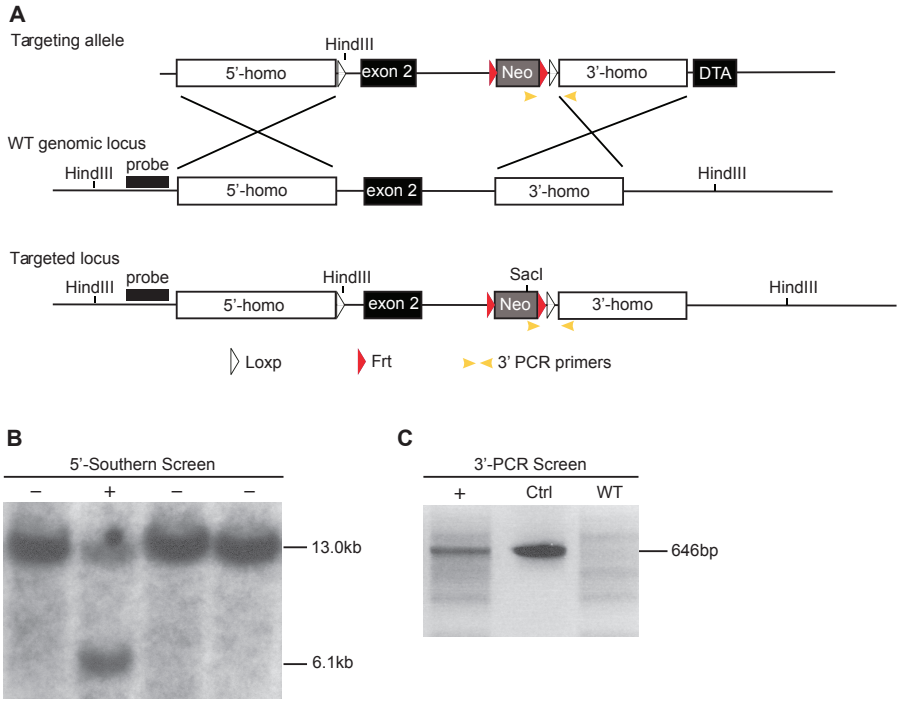
A
Targeting allele
HindIII
5'-homo
exon 2
Neo
3'-homo
DTA
WT genomic locus
HindIII
probe
5'-homo
exon 2
3'-homo
HindIII
Targeted locus
HindIII
probe
HindIII
SacI
5'-homo
exon 2
Neo
3'-homo
HindIII
Loxp
Frt
3' PCR primers
B
5'-Southern Screen
–
+
–
–
13.0kb
6.1kb
C
3'-PCR Screen
+
Ctrl
WT
646bp

Figure 2.1. Generating the *Has2* conditional knockout allele *Has2^{fl}*.

(A) Illustration of *Has2* conditional knockout targeting construct with two LoxP sequences flanking exon2, which include the ATG translation initiation codon and N-terminal of *Has2* protein. A *frt-neo-frt* cassette was also inserted for positive selection. PGK driven diphthera toxin (DTA) was incorporated into the targeting vector to increase the efficiency of homologous recombination in ES cells. The location of DNA probe is indicated by thick black bar situated outside of 5' homologous arm whereas yellow arrowheads represents the location of PCR primers.

(B) Southern blotting was initially used to screen homologous events using the DNA probe. Genomic DNA was digested with HindIII and the correct targeted locus (+) is represented by the 6.1 kb fragment whereas the non-targeted locus (-) shows 13 kb on the Southern blot.

(C) PCR was subsequently used to confirm homologous event at 3' end of *Has2* locus. The location of the primers are designed such that only targeted locus will be amplified as a 646 bp fragment. Primers for PCR are forward: 5'-TATTGCTGAAGAGCTTGGCGG-3' and reverse: 5'-AAGAAGAGACAGAGCCTGCC-3'.

The probes used were *Has2* (IMAGE:30533251), *Gdf5* (IMAGE:4190036), *Wnt4* (Gavin et al., 1990), *Chordin* (Klingensmith et al., 1999), *Sox9* (Ng et al., 1997), *Noggin* (McMahon et al., 1998), *Col2a1* (Ng et al., 1997) and *Pgk1*(IMAGE:6828087). Immunohistochemistry on paraffin-embedded sections were performed as previously described (Li et al., 2004). For detection of aggrecan and link protein, tissue sections were first treated with 0.1% trypsin for 10 minutes at 37 °C for enzymatic antigen retrieval, and then with chondroitinase ABC (0.25 unit/ml; Sigma) for 30 minutes prior to incubation with the primary antibodies. The primary antibodies were rabbit anti-phosphorylated Erk1/2 (Cell signaling, 1:200), rabbit anti-cleaved Caspase 3 (Cell Signaling, 1:200), rabbit anti-phosphorylated Histone 3 (Millipore, 1:1000), mouse anti-CSPG (DSHB, 9BA12, 1:10), mouse anti-aggrecan (DSHB, 12/21/1-C-6, 1:10) and mouse anti-link protein (DSHB, 9/30/8-A-4, 1:10).

Chromatin immunoprecipitation (ChIP)

The *RosaGli3T*$^{Flag\ c/c}$ line, which contains a Cre-inducible 3XFlag-tagged Gli3 repressor (Vokes et al., 2008), was crossed with homozygous *Prx1Cre* mice (Logan et al., 2002). For each ChIP experiment, we collected forelimbs and hindlimbs from a single litter of eight or nine E11.5 embryos and performed ChIP with the M2 anti-Flag monoclonal antibody (Sigma) as described previously (Vokes et al., 2007; Vokes et al., 2008), performing a total of three independent experiments. For a negative control, limb buds were dissected from a single litter of E11.5 wildtype Swiss Webster embryos and ChIP was performed using the same anti-Flag antibody. The occupancy of Gli3 repressor on the *Has2* locus was measured by realtime q-PCR using primer sets targeting different loci

of the *Has2* promoter region. q-PCR was performed in 20ul reaction containing SYBR Green Master Mix (ABI), and ran on the ViiA7 Real-Time PCR System (ABI). The primer sets used were: P1: primer set#1, Forward CTCATGGCAATGGGTTTTCT and Reverse TGCATGATATGCAGTCCACA; P2: primer set#2, Forward AGAGGGGAGAACCAAGCATT
and Reverse AGGGTCGTGGAAGGAAGTTT; P3: primer set#3, Forward CAAGGATTCCCTCGACTTGA and Reverse CACGGACGTACACACACACA; P4: primer set#4, Forward GGCTGGACACTGAAATGAGG and Reverse AAGGCTGTCAAGAGGCAAAA; P5: primer set#5, Forward CTTGTGGGCATTTAGGCATT and Reverse TCAGACCTGAGCTTCCTGGT; P6: primer set#6, Forward CATGGAAGCCAGAAGAGGTT and Reverse AGCATGCCAAGATCCTATGC; Gli1 Gli3-ChIP site, Forward GGACAAAGAGACCTGGGACA and Reverse AGGAGATGCTCTGACGCCTA; Ptch1 Gli3-ChIP site, Forward AGGCCTGCACCAATAATGAC and Reverse TCCTTGCTCGCCTCTTTAAC; Baseline,
Forward CTGGCCTCCATACACACATA and Reverse AGTCAGCAGGATCCACACTT. The enrichments were calculated by the delta(delta)Ct method and the enrichment levels of each primer set are shown as Log2 values.

Cell-based luciferase reporter assay

The 2880bp promoter sequence (mm9|chr15:56525549-56528428) of *Has2* was generated by PCR and cloned upstream of the luciferase reporter in pGL3 Basic plasmid (Promega, WI). Primers used were as follows: Forward:

ttgtctcgagTATGAATGCATCAACGATAAACG and Reverse: atttaagcttCTTGTTCAGCTCCTGCTCATAGA. Mutations at putative Gli binding sites (M1: GCCCACCCA to GCCagCtgA; M2: GACCACACA to GACagCtgA) were generated using QuikChange mutagenesis kit (Stratagene, CA). Luciferase assays were performed essentially as previously described (Huang et al., 2010), using the Promega Dual Luciferase Reporter Assay system (Promega, WI). All reporter assays were normalized using Renilla luciferase as internal control. Each data point represents the mean of triplicate wells with error bar representing the standard deviation (SD).

Skeletal staining

Whole-mount skeletal staining with Alcian blue and Alizarin red to visualize cartilage and mineralized bone was performed as described (Chiang et al., 2001).

Micromass culture

Micromass cultures were prepared from E11.5 hindlimbs as previously described (Ahrens et al., 1977; James et al., 2005; Stanton et al., 2004). Dissociated cells were resuspended in growth medium at a concentration of 2 x 10^7 cells/ml and spotted as 10ul droplets onto 24-well plates. Cells were allowed to adhere for 2 h at 37 °C, then 500 ul of 1:1 DMEM/F-12 medium containing 10% FBS was added. Growth medium was replaced every other day. At day 7 after seeding, micromass cultures were collected for Alcian blue staining or *Col2a1* micromass whole mount in situ hybridization according to published methods (Cash et al., 1997).

EF5 staining

Pregnant females were i.p. injected with 10 mM EF5 (gift of NCI through Dr. Cameron Koch, University of Pennsylvania) in 5% dextrose and 2.4% ethanol, with an amount equal to 1/100 of the animal weight (1ml/100g). Two hours after injection, embryos were collected and embedded in OCT freezing medium. 10 um frozen sections were collected and fixed in freshly prepared 4% PFA for 60 minutes. Slides were rinsed in PBST (PBS+0.3% Tween 20) three times and blocked in PBST containing 2% milk and 5% goat serum at 4C overnight. Block solution was removed by dipping slides in PBST and stained for 6 hours in 100ul Alexa 488-conjugated ELK3-51 (anti-EF5) antibody solution (obtained from Dr. Cameron Koch). The slides were rinsed in PBST 3 times and mounted in FluorSave (Millipore, MA) for fluorescent imaging.

Results

Has2 expression in the posterior limb bud mesenchyme is dependent on Shh signaling.

In an effort to identify downstream targets of Shh signaling, we performed microarray analysis on an Affymetrix Exon array using total RNAs extracted from the anterior and posterior halves of E10.5 mouse limb buds (Fig. 2.2A). We identified *Hyaluronan Acid Synthase 2* (*Has2),* which was upregulated 1.35 fold in the posterior limb, as a candidate gene regulated by Shh signaling. In this screen, other known Shh target genes that were upregulated in the posterior limb include *Ptch1* (2.23 fold) and *Gli1* (1.54 fold). RT-PCR analysis confirmed the enriched posterior expression of *Has2* in developing limb buds, as were *Shh* and *Gli1* (Fig. 2.2B). RNA *in situ* hybridization revealed that *Has2* mRNA expression starts as early as E9.5 and its dynamic expression domain expands with limb growth but is restricted posteriorly from E9.5 to E11.5 (Fig. 2.2C-J), although low level expression in the proximal region adjoining the body wall can be detected (* in Fig. 2.2C, G, K). *Has2* expression in the hindlimb was consistently lower than that in the forelimb, which is in agreement with the fact that there is ~12-hour delay in the development of the hindlimb compared to forelimb. To determine whether *Has2* expression is dependent on Shh signaling, we examined *Has2* mRNA expression in $Shh^{-/-}$ mutants. *Has2* expression is either absent or dramatically reduced in $Shh^{-/-}$ mutant limb buds at E10.5 (Fig. 2.2M, N) and E11 (Fig. 2.2Q, R) whereas its most proximal expression abutting the body wall remains (* in Fig. 2.2M, Q). Similarly, at E12.5 *Has2* expression in the distal limb is largely absent but low level expression persists in the proximal region of the autopod (Fig.

2.2Y, Z). These observations strongly suggest that early *Has2* expression depends on Shh signaling.

Has2 expression in the anterior limb bud is suppressed by Gli3 repressor.

The patterning function of Shh is mainly mediated by Gli3 in the limb. In the presence of Shh signaling, the full-length form of Gli3 protein (Gli3-FL) is activated and functions as a transcriptional activator (Gli3A). In the absence of Shh signal, as in the anterior limb bud, Gli3-FL is cleaved into a repressor form (Gli3R) where it suppresses the expression of Shh-responsive genes (Litingtung et al., 2002; te Welscher et al., 2002). By examining *Has2* mRNA expression in *Gli3*^{xt} mutants, which lack Gli3 function, we identified an ectopic expression domain in the anterior margin of the limb underlying the AER (Fig. 2.2S, T, arrows), indicating that Gli3R represses *Has2* expression in the anterior limb. This ectopic *Has2* expression persisted *in Shh*$^{-/-}$*;Gli3*^{xt} double mutants (Fig. 2.2U, V, arrows), suggesting that activation of anterior *Has2* expression does not require Shh pathway activation and can be activated by Gli3R derepression. However, the posterior expression of *Has2* in *Shh*$^{-/-}$*; Gli3*^{xt} double mutant limbs was reduced, suggesting a GliA contributes quantitatively to normal expression levels (Fig. 2.2U, V). Together, these data suggest that Gli activators and Gli3R regulate *Has2* expression in the limb.

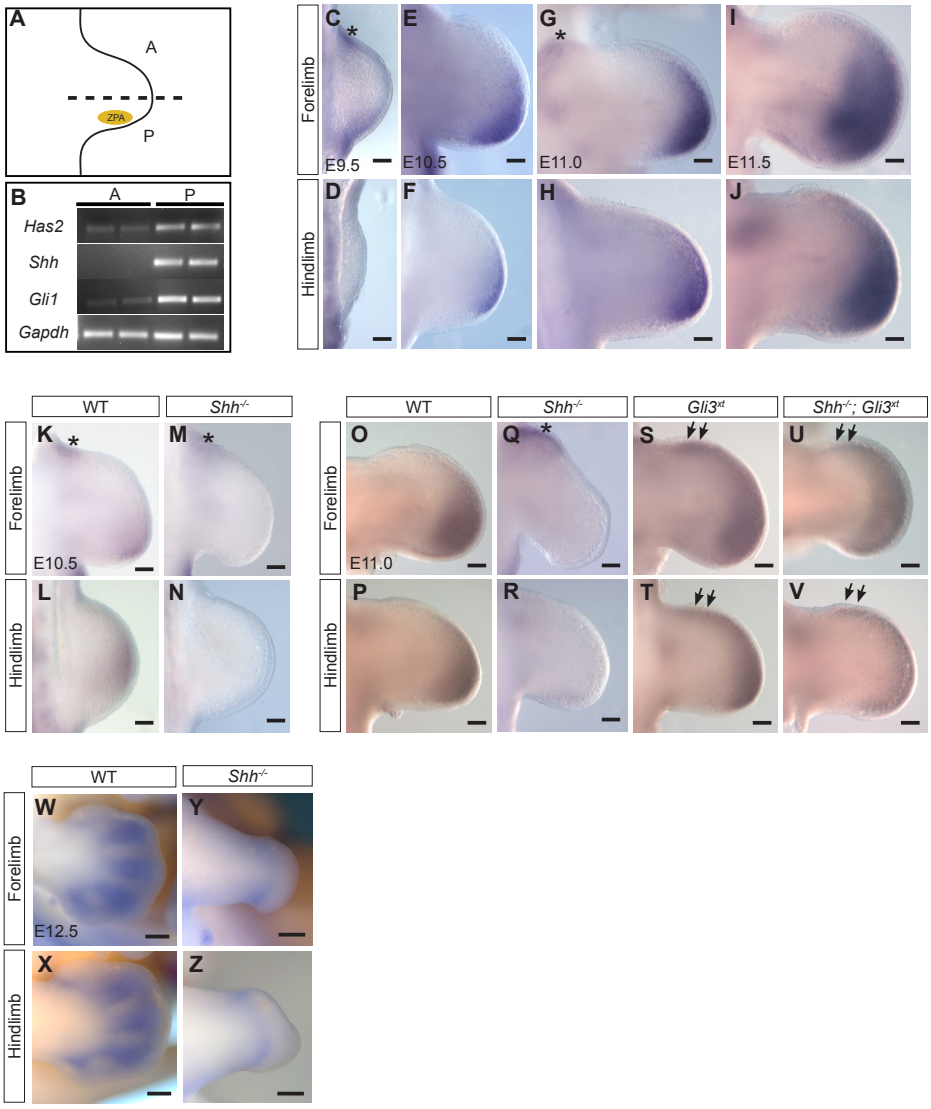
A
A
ZPA
P
B
A
P
Has2
Shh
Gli1
Gapdh
Forelimb
Hindlimb
C
E
G
I
D
F
H
J
E9.5
E10.5
E11.0
E11.5
WT
Shh-/-
Gli3xt
Shh-/-; Gli3xt
K
M
O
Q
S
U
L
N
P
R
T
V
E10.5
E11.0
W
Y
X
Z
E12.5

Figure 2.2. *Has2* is regulated by Shh signaling in the limb bud.

(A) E10.5 limb illustration with posterior domain (P), anterior domain (A) and the Zone of polarizing activity (ZPA). For anterior versus posterior tissue analysis, the limb was bisected at the midline (dotted line). (B) RT-PCR of anterior and posterior halves of limb buds showing increased expression of *Shh*, *Gli1* and *Has2* in the posterior domain. *Has2* expression in mesenchyme of forelimb (C, E, G, I) and hindlimb buds (D, F, H, J) from E9.5 to E11.5 by whole mount RNA *in situ* hybridization. Posterior *Has2* expression is undetectable in E10.5

$Shh^{-/-}$ (M, N) compared with WT (K, L) limb buds. At E11, posterior *Has2* expression is barely detectable in $Shh^{-/-}$ (Q, R) compared with WT (O, P) limb buds. *Has2* expression is expanded anteriorly in $Gli3^{xt}$ mutant limb buds at E11 (S, T, arrows) compared with wildtype (O, P). Note diminished *Has2* mRNA in posterior limbs of $Shh^{-/-};Gli3^{xt}$ double mutants while expanded anterior *Has2* remains comparable to $Gli3^{xt}$ limbs (U, V, arrows). Low level *Has2* expression in the most proximal region adjoining the body wall can be detected in WT (C, G, K, *) and this expression is unaltered in $Shh^{-/-}$ (M, Q, *). (W-Z) At E12.5, *Has2* expression is mostly confined to the condensing digit mesenchyme (W, X), and this patterns of expression is largely absent in Shh mutants although low level *Has2* expression persists in the proximal region of the autopod (Y, Z). Scale bar, 75 microns.

Has2 is a direct target of Gli transcription factors

Based on our genetic data, we hypothesized that Shh signaling directly regulates *Has2* expression in early limb development. The Gli transcription factors are Shh signaling effectors and have DNA binding zinc finger domains to bind to the consensus sequence TGGGTGGTC on target genes to initiate or suppress transcription (Hallikas et al., 2006; Kinzler and Vogelstein, 1990; Vokes et al., 2007; Vokes et al., 2008; Vortkamp et al., 1995). Through *in silico* analysis, we identified two such consensus sequences within the 3 kb *Has2* regulatory region, one at -646bp (Gli-binding site 1,GBS1) and the other at +504bp (GBS2) from the *Has2* transcriptional start site (+1) (Fig. 2.3A, B). To determine if these binding sites are capable of responding to Gli1 activation, we generated *Has2* reporter constructs by cloning the ~3 kb *Has2* promoter fragment upstream of the luciferase gene (Fig. 2.3B, C). The *Has2* reporter, either unaltered or containing mutation at one or both GBSs (Fig. 2.3C), was then co-transfected with *Gli1*-expressing or control vector into Shh-responsive 3T3 cells (Taipale et al., 2000). Consistent with the presence of GBSs, we observed significant induction of luciferase activity by Gli1 (Fig. 2.3D). Importantly, mutations in either or both GBSs reduced reporter activity to basal level, indicating that these sites are necessary for Gli1 activation and may function cooperatively (Fig. 2.3D).

We next performed transgenic analysis to further characterize the *Has2* promoter fragment and found that it contains the necessary cis-regulatory elements to direct expression of a reporter gene in the posterior limb mesenchyme (Fig. 2.3E), revealing the relevance of this region in the context of limb development and Shh regulation.

To determine whether Gli can directly bind to GBSs at the *Has2* promoter region *in vivo*, we utilized *Prx1-cre; RosaGli3T*$^{Flagc/c}$ transgenic embryos in which FLAG-tagged Gli3 repressor is expressed under the control of ubiquitous *Rosa26* promoter which is selectively activated in the early limb mesenchyme by *Prx1-cre* (Vokes et al., 2008). We designed several q-PCR primer sets within the *Has2* regulatory region, P1 through P6 (Fig. 2.3B), and performed ChIP using antibody against the FLAG epitope followed by q-PCR analysis on Gli3-bound chromatin to determine enrichment of PCR products. Regions spanning the two GBSs (P2, P3, P4) were enriched by 40-80 fold, similar to enrichment for known Gli target genes *Gli1* and *Ptch1* (Fig. 2.3F). In contrast, regions tested that were outside the GBSs either ~2.8kb upstream (P1) or 3.0kb downstream (P6) showed no enrichment, indicating that Gli binds directly to this regulatory region of *Has2 in vivo* (Fig. 2.3F). This is consistent with Gli3T binding observed at this site in a previously published genomic dataset (Vokes et al., 2008).


A
GBS1
GBS2
mouse
Rat
Human

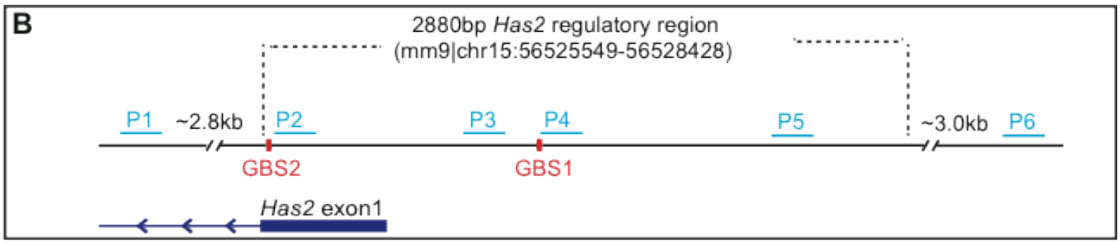
B
2880bp Has2 regulatory region
(mm9|chr15:56525549-56528428)
P1
~2.8kb
P2
P3
P4
P5
~3.0kb
P6
GBS2
GBS1
Has2 exon1

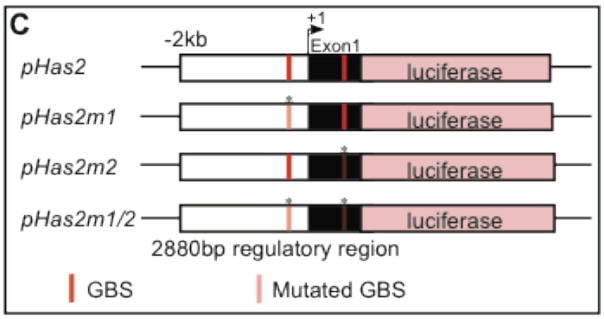
C
-2kb
+1
Exon1
pHas2
pHas2m1
pHas2m2
pHas2m1/2
luciferase
2880bp regulatory region
GBS
Mutated GBS

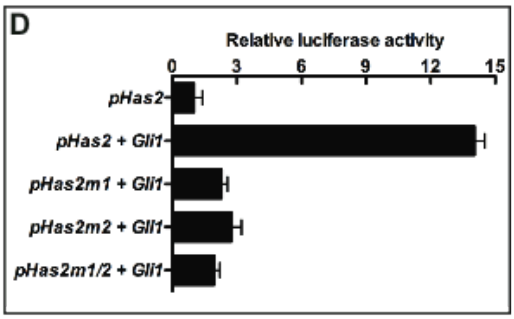
D
Relative luciferase activity
0
3
6
9
12
15
pHas2
pHas2 + Gli1
pHas2m1 + Gli1
pHas2m2 + Gli1
pHas2m1/2 + Gli1

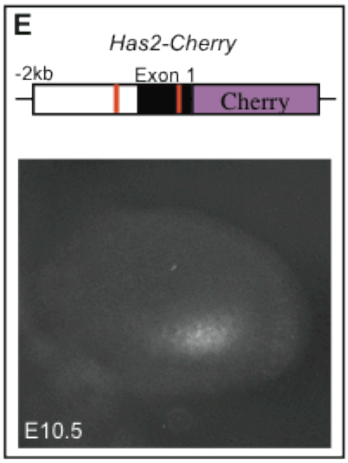
E
Has2-Cherry
-2kb
Exon 1
Cherry
E10.5

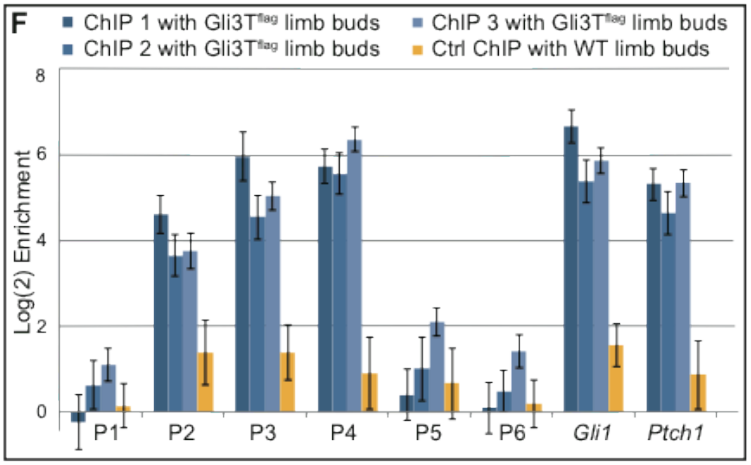
F
ChIP 1 with Gli3T^flag limb buds
ChIP 2 with Gli3T^flag limb buds
ChIP 3 with Gli3T^flag limb buds
Ctrl ChIP with WT limb buds
Log(2) Enrichment
8
6
4
2
0
P1
P2
P3
P4
P5
P6
Gli1
Ptch1

Figure 2.3. Gli transcription factors directly regulate *Has2* promoter activity.

(A) Prediction *in silico* identified two potential Gli-binding sites, which are highly conserved in mammals, in the *Has2* promoter. (B) Illustration of genomic *Has2* regulatory region; ~3.0kb *Has2* regulatory region was used for luciferase assays. P1 through P6 were target sequences used to identify in vivo Gli binding by chromatin immunoprecipitation (ChIP). Note that the 5' untranslated region (5'UTR) spans exon 1 of *Has2*. (C) Reporter constructs used in luciferase assays. ~3.0kb *Has2* regulatory region was subcloned into pGL3 luciferase plasmid (*pHas2*). Potential Gli binding motif was singly mutated (*pHas2m1*, *pHas2m2*) or doubly mutated (*pHas2m1/2*). (D) Normalized luciferase values obtained when 3T3 cells were cotransfected with various derivatives of *Has2* luciferase reporter with or without *Gli1* expression construct. (E) ~3 kb *Has2* promoter is sufficient to direct Cherry reporter expression in the posterior limb mesenchyme. (F) *FlagGli3* ChIP for in vivo detection of Gli3 binding to *Has2* promoter. Regions spanning the two potential Gli binding motifs (P2, P3, P4) are substantially enriched by 40-80 fold, similar to enrichment for positive control loci *Gli1* and *Ptch1*. The positive control regions are validated Gli3 binding regions near the *Gli1* and *Ptch1* loci (Vokes et al., 2008). ChIP1, ChIP2, ChIP3 represent three independent biological samples of anti-Flag ChIP using E11.5 *Prx1Cre; RosaGli3T*$^{Flagc/c}$ limb buds. Ctrl ChIP represents same stage wildtype limb buds. All assays were performed in triplicate and error bars represent the standard error of mean.

Has2 conditional mutants display mispatterning of joints and defective chondrogenesis

To elucidate the role of Shh-induced *Has2* in early limb development, we generated a *Has2* conditional knockout allele ($Has2^{fl}$) to circumvent the early lethality of *Has2* null mutants (Camenisch et al., 2000)(Fig. 2.1). We selected *Hoxb6-cre* to inactivate *Has2* function in the early limb mesenchyme based on the observations that *Hoxb6-cre* is more effective than *Prx1-cre* in abrogating gene function in early limb buds when crossed to various conditional mutants (Li et al., 2005; Lowe et al., 2000; Scherz et al., 2007; Yu and Ornitz, 2008; Zhu et al., 2008). Because the rostral limit of *Hoxb6* expression domain is confined to the posterior forelimb, all analyses were performed in hindlimbs except where noted. Indeed, skeletal preparation of newborn $Hoxb6^{Cre};Has2^{fl/-}$ ($Has2^{cko}$) hindlimbs showed much more severe phenotype than previously described (Fig. 2.4A, B) (Matsumoto et al., 2009). Focusing on the digits, the mutants displayed longitudinally oriented cavities that split proximal and medial phalanges (Fig. 2.4E, E' versus F, F'). As expected, the digit defect in the forelimb is restricted to the posterior digits (Fig. 2.4C, D), consistent with restricted Cre expression. Histological staining at E16.5 showed that the space adjoining the split phalanges is occupied by distinct loosely associated mesenchymal cells that are reminiscent of cells at interphalangeal joints (Fig. 2.4 G, G' versus H, H'). Additionally, the mutant digits displayed disorganized cartilage nodules, suggesting a role of *Has2* in chondrogenesis (Fig. 2.4F, F', H, H'). Consistent with this finding, limb micromass cultures of $Has2^{cko}$ followed by Alcian blue staining or *Col2a1* (type II collagen) expression revealed striking loss of cartilage-forming potential (Fig. 2.4 I, J and K, L).

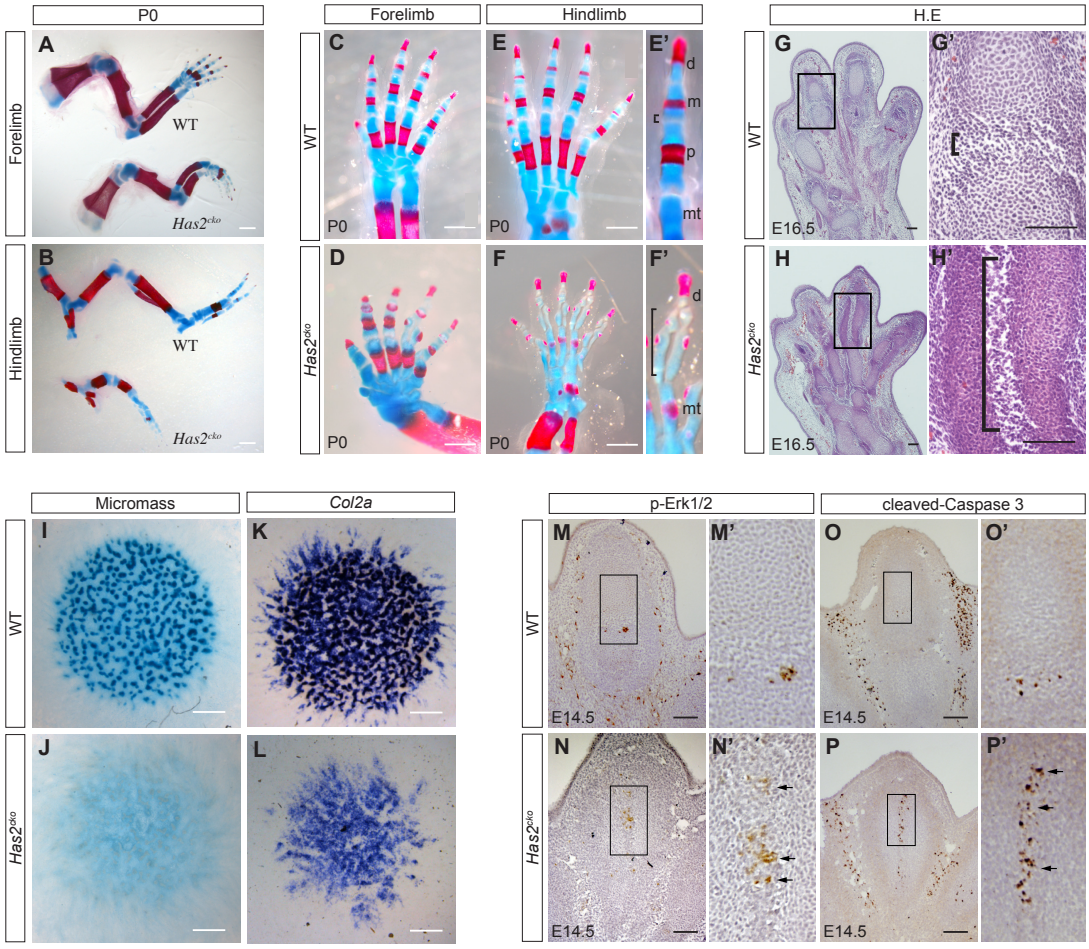
P0
Forelimb
Hindlimb
A
B
WT
Has2cko
Forelimb
Hindlimb
C
D
E
F
E'
F'
WT
Has2cko
P0
d
m
p
mt
H.E
G
G'
H
H'
E16.5
Micromass
Col2a
I
J
K
L
p-Erk1/2
cleaved-Caspase 3
M
M'
N
N'
O
O'
P
P'
E14.5

Figure 2.4. *Has2*^{cko} mutant hindlimbs display chondrogenesis and joint positioning defects

Whole-mount skeletal elements of P0 wild-type and *Has2*^{cko} forelimbs (A) and hindlimbs (B) stained with Alizarin red and Alcian blue. Severe cartilage reduction and joint positioning defect are apparent in P0 *Has2*^{cko} digits (D, F, F') when compared to wildtype (C, E, E'); note that interphalangeal joints highlighted by brackets are perpendicularly shifted in *Has2*^{cko} mutants. Hematoxylin and Eosin staining of E16.5 hindlimb sections (G, H), with higher magnification view of joint cavities (G', H'). In addition to aberrant joint formation, the mutants (H, H') also show prominent change in phalangeal cartilage nodule organization indicating defective chondrogenesis. *Has2*^{cko} limb micromasses J, L) show reduced chondrocyte differentiation while wildtype (I, K) display robust capacity to differentiate as shown with Alcian blue staining (I, J) and *Col2a* expression (K, L). Sections of E14.5 digits immunostained with p-Erk1/2 (M, N) and cleaved-Caspase 3 (O, P) showing ectopically expanded expression of p-Erk in *Has2*^{cko} digits (N', arrows) and likewise cleaved Caspase 3 is also expanded (P', arrows). Note that this orthogonally shifted pattern in *Has2*^{cko} agrees with the ectopic positioning of *Gdf5*-expressing joint cells (G' versus H'). In contrast, wildtype littermates show p-Erk (M, M') and cleaved Caspase 3 (O, O') expressions confined to cells in the normal joint interzone (M', O'). Scale bar, 500 microns (white) and 50 microns (black)

The first histological indication of synovial joint formation is the appearance of flattened cells at a stereotypic joint location known as the interzone at ~E12.5 in mouse digits. As development proceeds, the interzone undergoes cavitation, a process where physical separation of opposing skeletal elements occurs (Khan et al., 2007). While the mechanism involved in joint forming activities remains to be fully deciphered, both programmed cell death and Erk activation have been implicated in this process (Fernandez-Teran et al., 2006; Pitsillides, 2003; Pitsillides and Ashhurst, 2008; Seo and Serra, 2007). Because *Has2*^{cko} mutants displayed perpendicularly oriented joint cavities in the digits, we sought to determine whether there was a similar shift in the expression pattern of pErk and cleaved Caspase 3 for cell death. At E14.5, p-Erk (Fig. 2.4M, M') and cleaved Caspase-3 (Fig. 2.4O, O') immunoreactivities are normally restricted to the joint perpendicular to the digit shafts but these expressions were mislocalized along the longitudinal axis in *Has2*^{cko} mutant digits (Fig. 2.4N, N', P, P'). Therefore, the disruption of *Has2* function leads to ectopic joints along the digit rays.

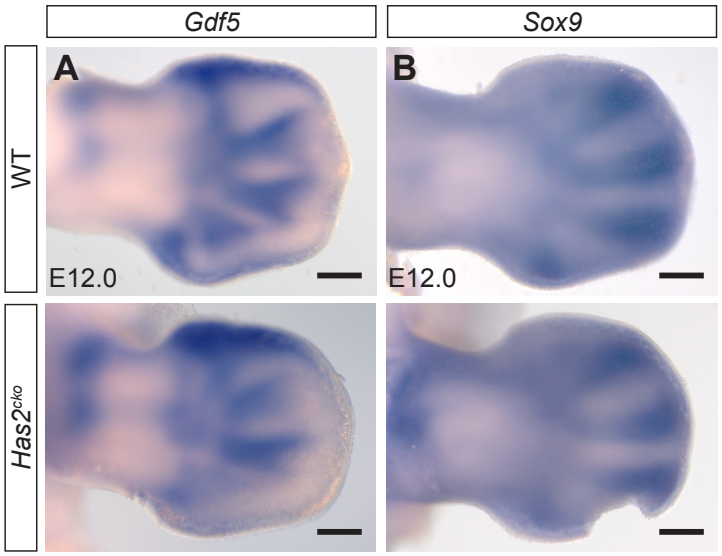

Figure 2.5. *Gdf5 and Sox9* expressions at E12 are not altered in *Has2^{cko}* hindlimbs.

Gdf5 expression in the perichondrium is comparable between wildtype (A) and *Has2^{cko}* mutant (B). Similarly, *Sox9* expression in chondrocyte progenitors is comparable between wildtype (C) and *Has2^{cko}* mutant (D). Scale bar, 150 microns

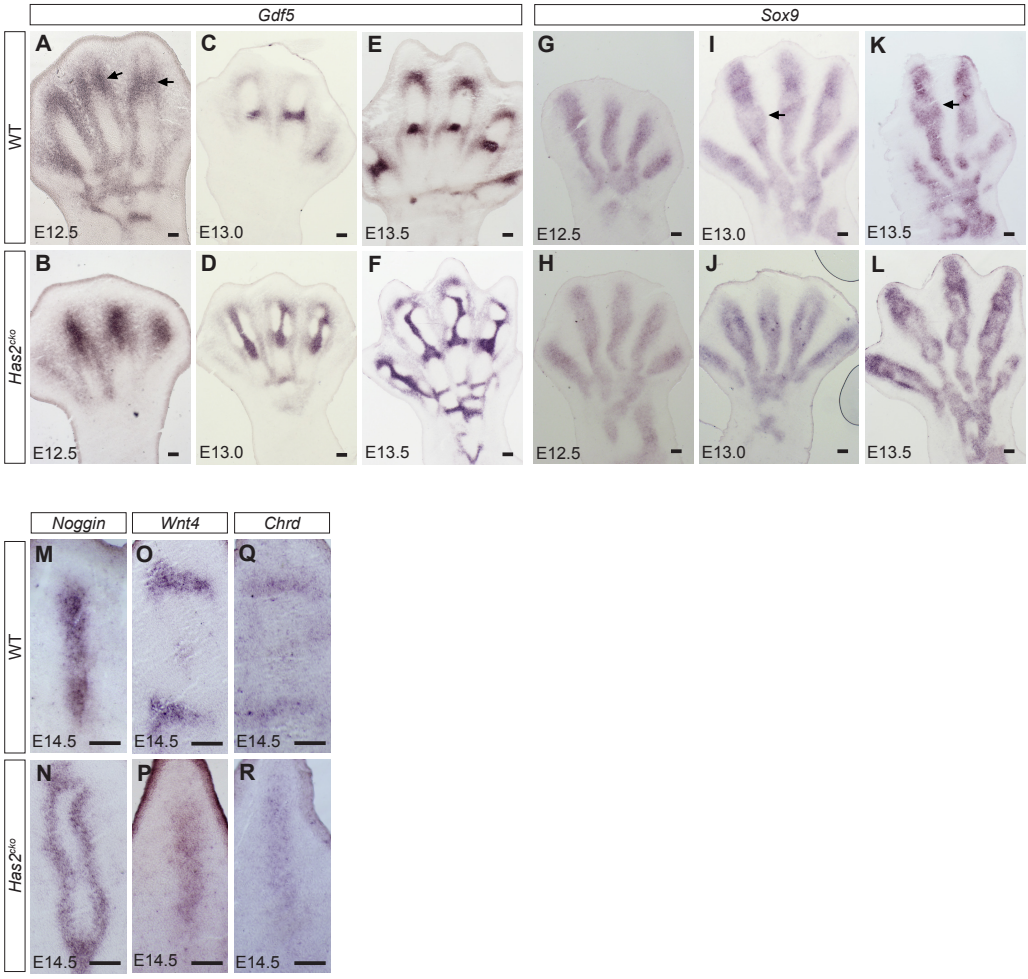
Gdf5
Sox9
WT
Has2cko
A
B
C
D
E
F
G
H
I
J
K
L
E12.5
E13.0
E13.5
Noggin
Wnt4
Chrd
M
N
O
P
Q
R
E14.5

Figure 2.6. Joint markers indicate aberrant positioning of the interzone in *Has2^{cko}*. Section *in situ* hybridization analysis for *Gdf5* (A-F) and *Sox9* (G-L) expression in wild-type (A, C, E, G, I, K) and *Has2^{cko}* (B, D, F, H, J, L) limbs. The joint defects in *Has2^{cko}* can be detected as early as E12.5 when *Gdf5* expression, which highlights the position of forming interzone (A, arrow), is expanded (B). The aberrant *Gdf5* expression becomes progressively more severe (C versus D) and by E13.5 the interzone is clearly orthogonally shifted in *Has2^{cko}* mutant limbs (E versus F). Similarly, *Sox9* expressions in the chondrocytic domain also highlight the defective interzone formation in *Has2^{cko}* (G-L). Arrows mark interzone where *Sox9* expression is absent, and this *Sox9* negative zone is expanded in *Has2^{cko}* digits. Similar to *Sox9*, *Noggin* expression is absent in the center of the condensing chondrocytes in *Has2^{cko}* digits but instead surrounds the orthogonally shifted joint (compare M and N). RNA *in situ* hybridization analyses showing ectopic expression of additional joint interzone markers, *Wnt4* and *Chordin*, in *Has2^{cko}* hindlimb digits (P, R) compared with wildtype (O, Q) at E14.5. Scale bar, 50 microns

Has2 is required for positioning the interzone

To evaluate the effect of *Has2* deficiency on joint development in detail, we examined the expression of *Gdf5,* an early joint-specific marker (Koyama et al., 2008; Storm and Kingsley, 1996). *Gdf5* expression in the autopod is first detectable at ~E12 in the perichondrium bordering the condensing digit rays (Storm and Kingsley, 1996)(Fig. 2.5). As development proceeds, perichondrial *Gdf5* expression diminishes while interzone expression becomes more prominent (Fig. 2.6A, C, E). In *Has2*^{cko} mutants, however, we observed much broader expression of *Gdf5* in the interzone at E12.5 (Fig. 2.6B) although perichondrial expression is initiated normally (Fig. 2.5). By E13, the aberrant *Gdf5* expression became more pronounced, as evidenced by longitudinal stripes of presumptive joint progenitors bisecting the proximal/medial phalanges and this pattern persisted throughout joint development (Fig. 2.6D, F).

The expression of other joint markers such as *Wnt4* (Fig. 2.6O, P) and *Chordin* (Fig. 2.6Q, R), were also altered in *Has2*^{cko} mutant hindlimbs as highlighted by longitudinal shift in their expression pattern when compared to control. *Noggin* expression in condensing cartilage also highlights the misplacement of phalangeal joints at E14.5 in *Has2*^{cko} hindlimbs (Fig. 2.6N) compared with wildtype showing clear demarcation of the joint region (Fig. 2.6M). Likewise, *Sox9* expression from E12.5-E13.5 in condensing cartilage mesenchyme highlights aberrant joint formation and longitudinal shift in *Has2*^{cko} (Fig. 2.6H, J, L) compared with wildtype joints (Fig. 2.6G, I, K; arrows showing normal joint location). We note that *Sox9* expression in digit rays in hindlimb buds of WT and *Has2*^{cko} at E12 were comparable suggesting that commitment of mesenchymal cells to the chondrocytic lineage was not affected by loss of *Has2* expression (Fig. 2.5). We also

determined the status of cell proliferation using mitotic marker phosphorylated-Histone H3 in E12.5 and E13.5 hindlimbs (Fig. 2.7). We did not find significant alteration in cell proliferation at these stages compared to wildtype when joint defects were already apparent in *Has2*^{cko} limb buds.

Disruption of CSPG-link protein-hyaluronan aggregates and impaired phalangeal mesenchymal condensation in *Has2*^{cko}

The profound joint patterning defects observed in our *Has2* conditional mutants are strikingly similar to mouse mutants that are either deficient in CSPG or imbalanced in proteoglycan sulfation (Sohaskey et al., 2008; Wilson et al., 2012). We therefore examined whether CSPG development is affected in *Has2*^{cko}. At pH 2.5, Alcian blue stains most acidic proteoglycans, while at pH1 only sulfated proteoglycans are stained (Lev and Spicer, 1964). We observed remarkable loss of Alcian blue pH1 staining in the *Has2*^{cko} condensing digit rays while the interdigital mesenchyme acquired Alcian blue staining at E12.5 (Fig. 2.8B and C, arrows), suggesting loss of CSPG integrity and its aberrant distribution in *Has2*^{cko} hindlimbs. Note that in the wildtype, Alcian blue staining is strong and confined to digits, with no apparent staining in the interdigital space (Fig. 2.8B, arrows). Similarly, CSPG immunostaining was strongly reduced in *Has2*^{cko} condensing digits when compared to control digits (Fig. 2.8E versus D). Moreover, we observed striking CSPG labeling in the interdigital mesenchyme in *Has2*^{cko} (Fig. 2.8E', arrow), which is not evident in wildtype (Fig. 2.8D', arrow), suggesting loss of tethering resulting in aberrant distribution of CSPG. This notion is in agreement with the fact that

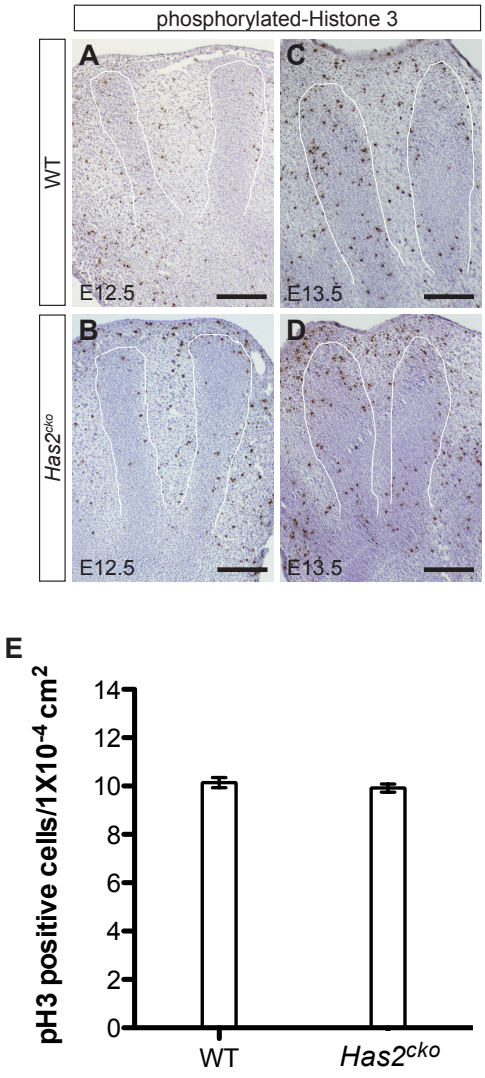

Figure 2.7. Mesenchyme proliferation is not significantly affected in *Has2*^{cko} limbs. Chondrocyte proliferation as indicated by phosphorylated Histone H3 immunostaining is not significantly different between wildtype (A, C) and mutants (B, D) at E12.5 (A, B) and E13.5 (C, D). (E) Quantification of p-H3 positive cells was carried from 3 pairs of wildtype and mutant limbs using unpaired student t-test. P=0.8155. Scale bar, 75 microns

HA is required for CSPG assembly and retention in the ECM (Day, 1999; Hardingham, 1979; Knudson, 1993; Kochhar et al., 1984; Maleski and Knudson, 1996b; Morgelin et al., 1994; Morgelin et al., 1988; Seyfried et al., 2005).

Aggrecan is a high molecular mass HA-binding CSPG abundant in cartilage pericellular matrix and forms an aggregate network with HA (Day, 1999; Hardingham, 1979; Hardingham and Fosang, 1992; Lee et al., 1993; Morgelin et al., 1994; Morgelin et al., 1988). Immunolabeling for aggrecan was reduced in the condensing digits (Fig. 2.8 F, G) but showed enhanced ectopic localization in the interdigital mesenchyme at E13.5 (Fig. 2.8F', G', arrows). Similarly, link protein, which stabilizes HA-aggrecan aggregates in cartilage (Watanabe and Yamada, 1999), was strikingly reduced in condensing digits and distributed aberrantly in the interdigital mesenchyme of *Has2*^{cko} limbs (Fig. 2.8H, I and H', I', arrows). Collectively, these findings highlight a crucial role for HA in assembling the pericellular CSPG matrix for proper mesenchymal condensation and subsequent interzone positioning.

Discussion

Chondrogenic differentiation and joint patterning in the developing vertebrate limb are dependent on cell-matrix interactions. Previous studies suggested that inductive signals regulate limb bud subridge mesoderm to maintain a relatively high rate of HA synthesis (Knudson and Toole, 1988). Consistent with this, bFGF was subsequently shown to stimulate HA synthesis in cultured chick embryonic limb mesodermal cells (Munaim et al., 1991). Other *in vitro* studies also showed that *Hyaluronan synthase* (*Has*) expression

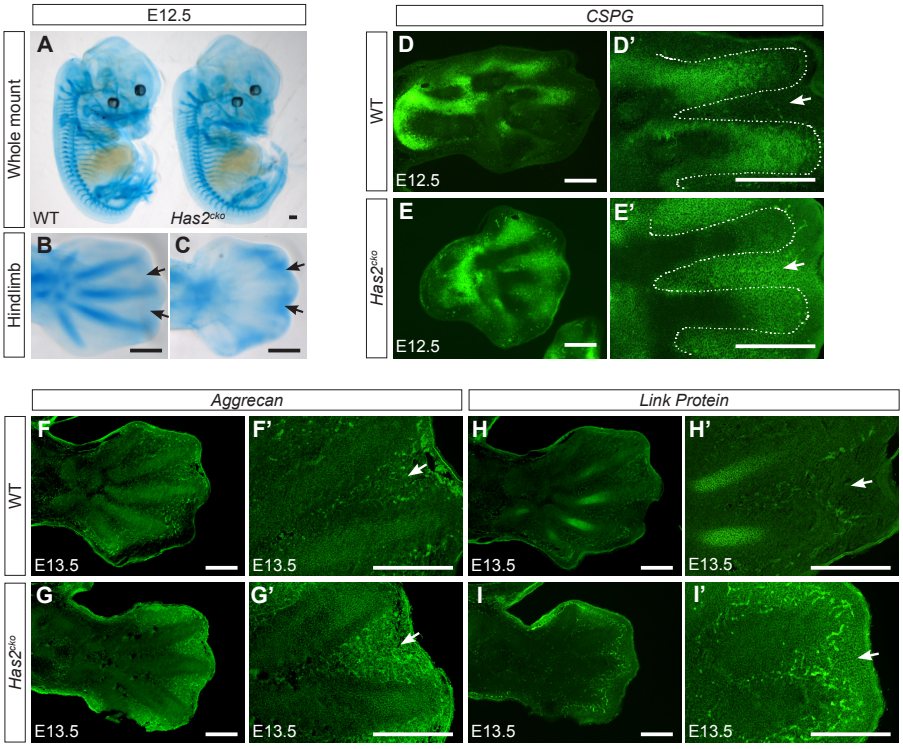
E12.5
CSPG
Whole mount
Hindlimb
WT
Has2cko
A
B
C
D
D'
E
E'
F
F'
G
G'
H
H'
I
I'
Aggrecan
Link Protein
E12.5
E13.5

Figure 2.8. Loss of *Has2* disrupts CSPG, aggrecan and link protein level and distribution.

Alcian blue staining of sulfated proteoglycans in E12.5 wild-type and *Has2*^{cko} embryos. Whole-mount preparation showed comparable staining except in the hindlimb (A). This is better shown in higher magnification view in which *Has2*^{cko} digits lack intense Alcian blue staining seen in wildtype (B) but show striking acquisition of staining in the interdigital regions (arrows in C). Immunostaining of *Has2*^{cko} (E, E', G, G', I, I') hindlimb sections compared with wild-type (D, D', F, F' H, H') for total CSPG (D, D', E, E'), aggrecan (F, F', G' G'), D') and link protein (H, H', I, I') showing markedly reduced expression of all these components, which normally form aggregates with HA, in *Has2*^{cko} hindlimb condensing digits (dotted line). CSPG is aberrantly distributed to the interdigital mesenchyme in *Has2*^{cko} limbs (compare arrow in D', E'), consistent with interdigital Alcian blue staining pattern in C, arrows. In contrast, CSPG is confined to condensing digits in wildtype with no apparent interdigital staining (arrow in D'). *Has2*^{cko} hindlimb buds also appear to have acquired interdigital staining for aggrecan (G', arrow) and link protein (I', arrow) which are confined to digits in wildtype. Scale bar, 150 microns

can be regulated by growth factors and cytokines (Jiang et al., 2011). However, the signal that induces the expression of *Has* during limb development is not known. Our study reveals that the molecular control of *Has2* gene expression in the early developing limb is Shh signaling. We demonstrated by genetic and molecular analyses that Shh signaling directly regulates *Has2* expression during early limb development. While *Has2* expression in the posterior limb mesoderm is dependent on both positive Shh induction and Gli3R derepression, its expression in the anterior mesoderm is induced by Gli3R derepression. It is interesting to note that *Has2* expression seems to occur in two phases in the developing autopod; early Shh-induced *Has2* at E9.5-12.5 (Fig. 2.2) and a late-induced phase at around E14.5-E16.5, likely independent of Hh, in presumptive joints and perichondrium where Hh pathway is not activated (Dy et al., 2010). Because aberrant interzone development occurs as early as E12.5 (Fig. 2.6B), we propose that the regulation of *Has2* by Shh signaling is important in digit joint patterning. However, our study cannot rule out the contribution of late-phase *Has2* expression in joint development. We note that residual *Has2* expression still persists in *Shh* mutant limbs (Fig. 2.2), which may explain the relatively normal expression of *Gdf5* in the single un-ossified digit 1 (Chiang et al., 2001).

Our finding imparts new insights into the role of Shh signaling in HA extracellular matrix induction which functions in tissue injury and repair (Jiang et al., 2007), and has long been implicated in tumorigenicity (Adamia et al., 2005; Bourguignon, 2008; Toole and Hascall, 2002; Whatcott et al., 2011). Has/HA has been implicated in epithelial transformation, support of the cancer stem cell niche, regulating tumor-stromal

interaction and growth and progression of a number of tumor types (Bernert et al., 2011; Bharadwaj et al., 2009; Kobayashi et al., 2010; Kosaki et al., 1999; Kramer et al., 2011; Li and Heldin, 2001; Li et al., 2007a; Okuda et al., 2012; Paiva et al., 2005; Simpson, 2006; Simpson et al., 2001; Simpson et al., 2002; Udabage et al., 2005; Zoltan-Jones et al., 2003). Our finding that Shh signaling induces *Has2*/HA expression can potentially be relevant in other developmental, injury or disease contexts where the Shh pathway is activated. Interestingly, *Rhamm* which encodes a hyaluronan-mediated motility receptor is also significantly upregulated in Shh pathway driven medulloblastoma (Read et al., 2009). In addition, *Has2* is upregulated in microarrays from Shh-driven cerebellar tumors (Chiang, unpublished observation). It remains to be determined if *Has2* is a target of Shh signaling uniquely during limb development or in the broader context of Shh-driven pathologies where the stromal microenvironment and extracellular matrix play critical roles in disease progression.

Our finding underscores the essential role of Shh signaling in regulating the composition and function of the early limb ECM scaffold, a novel finding that stands in contrast to its known role in promoting cell proliferation. We generated *Has2* conditional mutants to determine the significance of Shh-induced *Has2* during limb development. A previous study had shown that *Has2* is required for chondrocyte maturation and joint formation (Matsumoto et al., 2009). Our study is consistent with their findings, but provides additional insights regarding the role of *Has2* in CSPG complex assembly and digit patterning. We found that our *Has2* mutants displayed a more severe phalangeal phenotype, with orthogonal shifting of digit interzones that progressively developed into

joint cavities. This finding is strongly reminiscent of mutants that are defective in chondroitin sulfate synthesis or metabolism, and therefore underscores a central role of HA in the assembly of CSPG-aggregate complexes (see below). It is not entirely clear as to why our mutant phenotype is more severe than the previously reported *Has2* mutants. Because both alleles were designed to remove exon2, it is unlikely that there are allele differences. One possibility is that we used $Has2^{fl/-}$ as opposed to $Has2^{fl/fl}$ (Matsumoto et al., 2009). Alternatively, there is evidence to suggest that the *Prx-cre* line does not efficiently excise target sequences when compared to the *Hoxb6-cre* line prior to E10.5 (Li et al., 2005; Scherz et al., 2007; Yu and Ornitz, 2008; Zhu et al., 2008).

The limb bud mesenchyme synthesizes CSPGs in prechondrogenic condensations (Hascall et al., 1976; Shinomura et al., 1984; Tsonis and Walker, 1991). We observed early changes in the pattern and expression of CSPG, aggrecan and link protein with significantly less labeling indicating reduced and diffuse deposition in $Has2^{cko}$ condensing digits. This finding is consistent with the role of HA in assembling the HA-CSPG network stabilized by link proteins (Day, 1999; Hardingham, 1979; Hardingham and Fosang, 1992; Kohda et al., 1996; Lee et al., 1993; Morgelin et al., 1994; Morgelin et al., 1988; Seyfried et al., 2005). Various HA perturbation studies in limb cultures suggested that HA promotes assembly and retention of CSPG for pericellular matrix organization and HA plays a role in cell-cell adhesion and interaction during mesenchymal condensation (Knudson, 1993; Knudson et al., 1999; Knudson and Toole, 1985; Kochhar et al., 1984; Maleski and Knudson, 1996a, b). Recent findings *in vivo* provide evidence for the essential role of CSPG and link protein in chondrogenesis. Mice

deficient in CSPG biosynthesis developed skeletal dysplasia (Hiraoka et al., 2007). Abrogating *Chondroitin sulfate synthase* (*Chsy1*) or *Impad1*/*Jaws* resulted in impaired CSPG sulfation and defects in chondrocyte differentiation and maturation (Sohaskey et al., 2008; Wilson et al., 2012). Mutation of human *IMPAD1* leads to chondrodysplasia and joint abnormalities (Sohaskey et al., 2008; Vissers et al., 2011). Ablating link protein resulted in severe defects in chondrocyte organization, differentiation and maturation (Watanabe and Yamada, 1999). Indeed, our $Has2^{cko}$ limbs, with ectopic joints orthogonally shifted along the longitudinal axis, bear striking similarity to mutant limbs with impaired CSPG synthesis or sulfation (Sohaskey et al., 2008; Wilson et al., 2012), suggesting a central role of HA in the assembly of CSPG-aggregate complexes in vivo.

In addition to mutants that disrupt the composition of the ECM, inactivating *Hypoxia-inducible factor 1 α (Hif1α)* gene in the limb also produced longitudinal cavities representing aberrant joint patterning (Amarilio et al., 2007; Provot et al., 2007). However, the expression of the Hif1a target gene *Pgk1* or EF5 (a chemical probe for hypoxia) were not significantly changed in $Has2^{cko}$ limbs (Fig. 2.9). Together, these results suggest that the joint phenotype observed in $Has2^{cko}$ digits is not caused by changes in hypoxia regulation. While the precise mechanism by which *Has2* or CSPG deficiency leads to ectopic joint formation remains to be determined, it has been suggested that early *Gdf-5*-expressing cells migrate from the perichondrium region into the perimeter of developing cartilage (Pacifici et al., 2006; Storm and Kingsley, 1996). *Gdf5* is expressed in the perichondrium as well as interzone, and genetic fate mapping studies indicated that *Gdf5*-expressing cells contribute primarily to joint tissues

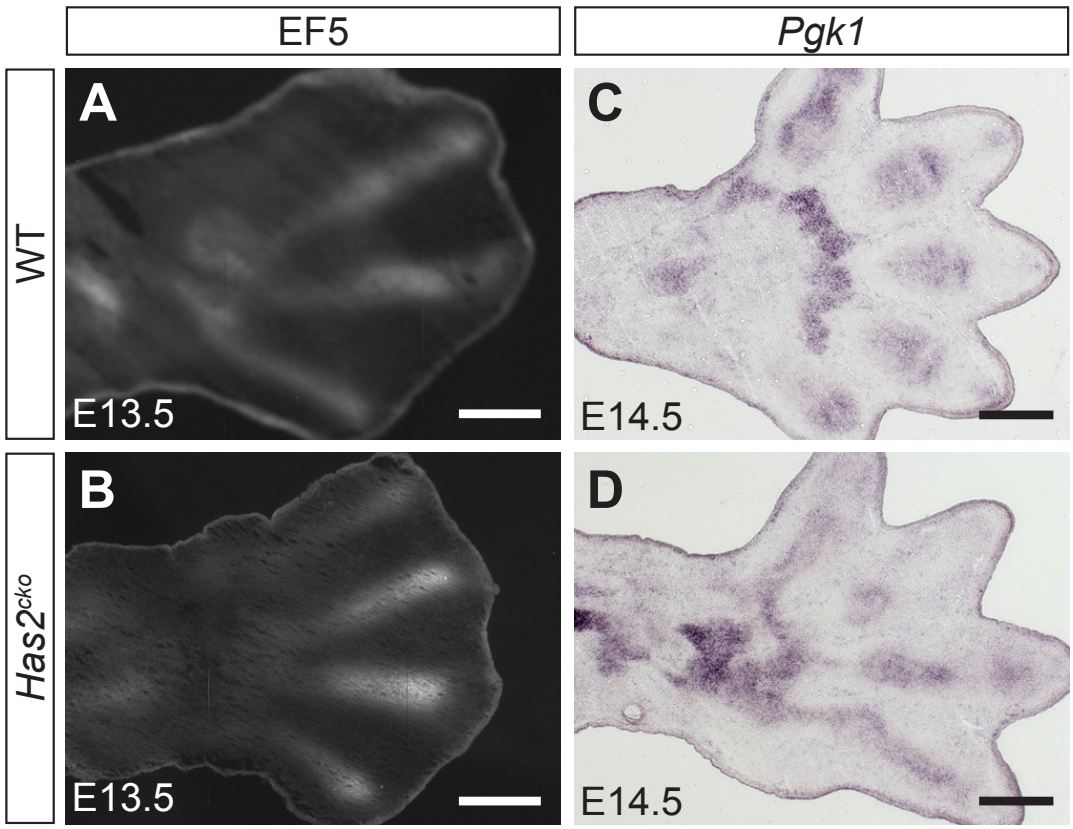

Figure 2.9. Hypoxia markers EF5 and *Pgk1* are not altered in *Has2*^{cko}

EF5 labeling (A, B) and *Pgk1* expression (C, D) in wildtype (A, C) and *Has2*^{cko} (B, D) hindlimbs. Scale bar, 150 microns

including articular cartilage and synovial lining (Koyama et al., 2008). Given that *Gdf5* expression in the perichondrium is initiated normally in *Has2*^{cko}, it is possible that disruption of HA-CSPG complex in condensing prechondrocytes may permit aberrant migration and subsequent positioning of interzone precursor cells. In summary, we have established *Has2* as a direct downstream target of Shh signaling pathway and demonstrated that it is required for interzone positioning. Our finding underscores the essential role of Shh signaling in regulating the composition and function of the early limb ECM scaffold, a novel finding that stands in contrast to its known role in promoting cell proliferation.

CHAPTER III

GENERAL DISCUSSION AND FUTURE DIRECTION

Since discovery of the *Drosophila Hh* gene more than thirty years ago (Nusslein-Volhard and Wieschaus 1980), and discovery thereafter of *Hh* homologs in vertebrates (Hammerschmidt et al., 1997; Ingham, 1998b), Shh signaling has become one of the hottest topics in biology drawing the attention and efforts of investigators from diverse research fields. Significant progress has been made in identifying the molecules of the Shh signaling cascade, which is mediated by three members of the Gli zinc-finger family of transcription factors (Ryan and Chiang, 2012; Weedon et al., 2008), as well as the roles of Shh signaling in a wide range of developmental processes such as limb development, central nervous system patterning and axon guidance (Ingham and McMahon, 2001; Jiang and Hui, 2008; Weedon et al., 2008). Recent studies have also implicated Shh signaling as essential for stem cell maintenance and cancer formation (Alison et al., 2012; Beachy et al., 2004; Kar et al., 2012; Wetmore, 2003; Zhao et al., 2009). Importantly, deregulation of Shh signaling contributes to numerous human disorders including Gorlin syndrome, Greig cephalopolysyndactyly syndrome, basal cell carcinoma and medulloblastoma (Bambakidis and Onwuzulike, 2012; McMahon et al., 2003; Nieuwenhuis and Hui, 2005).

In this study, I investigated the role of Shh regulation of a downstream target *Has2* during limb development. I revealed that posterior *Has2* expression is undetectable in $Shh^{-/-}$ limb

buds, indicating that *Has2* expression is under Shh signaling regulation. Through *in silico* screening analysis, we demonstrated the presence of two potential Gli-binding sites close to the mouse *Has2* promoter. Using mutational analyses, we established that Gli1 enhances *Has2* promoter activity via both putative Gli-binding sites in a cell-based assay. We also showed by ChIP analysis using Flag-Gli3R that Gli3R directly binds to both potential Gli-binding sites within the *Has2* regulatory region. Additionally, my studies using *Has2cko* mice have revealed that *Has2* is required for interzone positioning by stabilizing HA-CSPG complex in the extracellular matrix. Together, this work identifies *Has2* as a novel downstream target of Shh signaling required for joint patterning and chondrogenesis. This finding provides a novel link between Shh signaling and extracellular matrix stabilization during embryonic development.

The role of Has2 in A-P limb patterning

Functional analyses of *Gli* mutants suggest that Gli3 is the major effector of AP patterning in the limb. In the absence of Shh in the anterior limb, the full-length form of Gli3 protein (Gli3-FL) is cleaved and processed to a repressor form Gli3R, and attenuated in $Shh^{-/-}; Gli3^{xt/xt}$ double mutant, which lack all forms of Gli activators. Accordingly, *Has2* expression is anteriorly expanded in $Gli3^{xt/xt}$ mutants, which harbor null alleles of Gli3. Moreover, posterior expression of *Has2* is reduced in posterior limb in $Shh^{-/-}; Gli3^{xt/xt}$ double mutant. Thus, our studies strongly suggest that both Gli activator and repressor can regulate *Has2* expression in the limb. My study also indicated that AP patterning appears not to be regulated by *Has2*. Newborn $Has2^{cko}$ mice maintained a five-digit pattern in both fore- and hindlimbs, as confirmed by Alizarin red/Alcian blue

staining. LacZ staining in *Has2cko; NogginLacZ* embryos also confirmed that the order of digit formation was not altered (Fig. 3.1), suggesting that *Has2* itself is dispensable for specification of digit identity. Because *Has2* expression in the anterior limb mesoderm is repressed by Gli3R, it is still possible that anterior expansion of *Has2* may be involved in generating the polydactylous phenotype obserbed in $Gli3^{xt}$ mutants. To investigate whether *Has2* is required for the $Gli3^{xt}$ phenotype, I also generated $Has2^{cko}$*;* $Gli3^{xt}$ mutants and examined their digit phenotypes. To my surprise, $Has2^{cko}$*;* $Gli3^{xt}$ double mutants have 6 unassignable digits in the hindlimbs, the same digit pattern as in $Gli3^{xt}$ mutant (Fig. 3.2). This result indicates that loss of *Has2* cannot rescue the *Gli3* null phenotype, consistent with a lack of A-P patterning defect in *Has2* mutants.

Other potential targets of Hh signaling in the limb

In an effort to identify downstream targets of Shh signaling, we performed microarray analysis on an Affymetrix Mouse Exon 1.0 ST array using total RNAs extracted from the anterior and posterior halves of E10.5 mouse limb buds. From data mining, 377 transcripts were upregulated 1.5 fold or more in the posterior limb bud compared with the anterior limb bud. In contrast, 439 transcripts were enriched in the anterior limb bud 1.5 fold or more. The list of 377 includes well-characterized genes such as *Gli1, Shh, Ptch1, Msx1, Prdm1* (PR domain containing 1, with ZNF domain, aka PR domain zinc finger protein 1)*, Cck* (Cholecystokinin)*, Twist1, Gli3, Alx4* (Aristaless-like homeobox 4). Other genes, such as *Hoxd13, dHand, Grem1*, which are currently known to be regulated by Shh or Gli3R in the limb bud, were absent from the list of 377 (>1.5-fold) but were found in the list of genes that showed 1.2-1.5-fold change, indicating some limitation of the

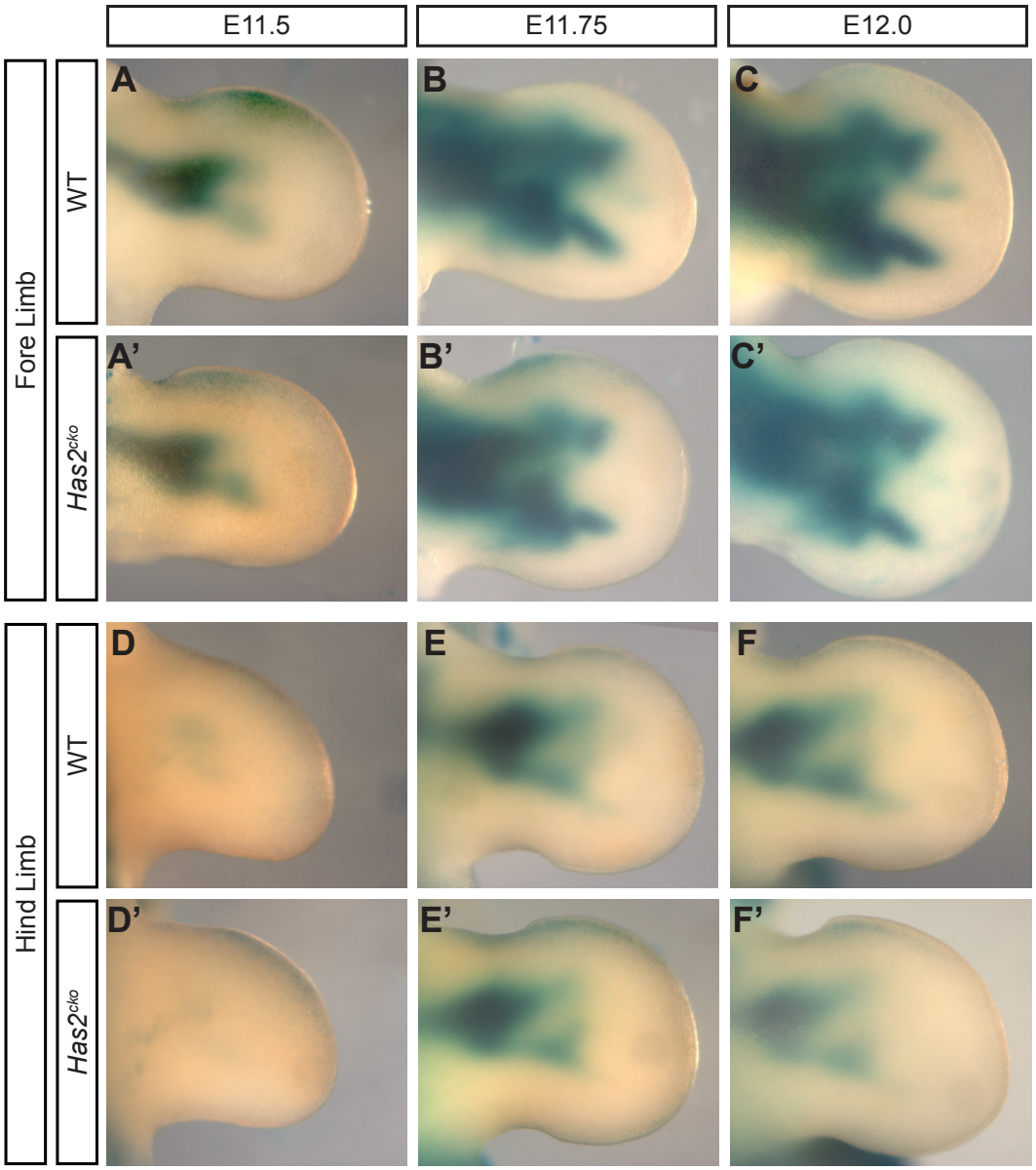

Figure 3.1. Sequence of digit formation is not altered in *Has2^{cko}* hindlimbs.

From E11.5 to E12.0, whole mount LacZ staining in the limb mesenchyme is comparable between wildtype; *Noggin^{LacZ}* (A-F) and *Has2cko*; *Noggin^{LacZ}* mutants (A'-F'), indicating the digit formation order is not altered in both forelimbs (A-C,A'-C') and hindlimbs (D-F, D'-F').

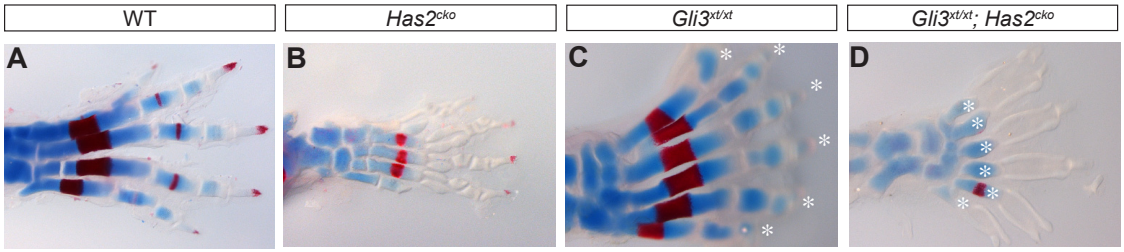

Figure 3.2. Loss of *Has2* cannot rescue *Gli3* mutant phenotype.

Skeletion preparation of E17.5 WT (A), *Has2*^{cko} (B), *Gli3*$^{xt/xt}$ (C), *Gli3*$^{xt/xt}$*; Has2*^{cko} double mutant (D) embryos. Alcian blue (Blue) staining to reveal cartilage. Alizarin Red staining (Red) to reveal bone. Note the *Gli3*$^{xt/xt}$*; Has2*^{cko} double mutant also display 6 indefinable digits (stars).

Microarray Analysis at the level of quantification. The microarray data has been deposited online at (http://www.ncbi.nlm.nih.gov/geo/query/acc.cgi?acc=GSE41691). Given that the downstream factors mediating Shh signaling during limb patterning remain largely elusive, further studies could focus on transcripts revealed by transcriptome profiling. Another genome-wide ChIP study using mouse limb buds derived from a transgene expressing an epitope-tagged Gli3 has identified over 200 putative direct Gli target genes (Vokes et al., 2008). Studying candidate genes that overlap in both profilings may unravel the functions of novel Shh signaling targets with crucial roles not only in limb development, but also in other tissues and organ systems with Hedgehog signaling activities. Several genes that appeared in both screens include *Aldh1a2* (Aldehyde dehydrogenase family 1, subfamily A2), *Calml4* (Calmodulin-like 4), *Cntfr* (Ciliary neurotrophic factor receptor), *Drd3* (Dopamine receptor D3), *Epha3* (Eph receptor A3), *Kcne4* (Potassium voltage-gated channel), *Nme2* (NME/NM23 nucleoside diphosphate kinase 2), *Osr1* (Odd-skipped related 1), *Prdm1* (PR domain containing 1, with ZNF domain, also known as PR domain zinc finger protein 1), *Rasgef1b* (RasGEF domain family, member 1B or GPI gamma-4), *Rspo3* (R-spondin 3 homolog, also known as cysteine-rich and single thrombospondin domain-containing protein 1 or roof plate-specific spondin-3); *Sall1* (Sal-like 1 or zinc finger protein Spalt-3) *and Smoc1* (SPARC related modular calcium binding 1, also known as secreted modular calcium binding protein 1). Of potential interest to Hh signaling and interactive pathways during tissue morphogenesis are Rspo3 and Smoc1. R-spondins (Rspo1-4) are secreted ligands that can activate Wnt/beta catenin signaling (de Lau et al., 2012)(Kim et al., 2008). It has been shown that Rspo3 amplifies Wnt signaling in the presence of Wnt ligand and coreceptor

Lrp6. Since Hh and Wnt signalings often operate concomitantly during tissue morphogenesis, understanding how Hh potentially modulates Rspo3 expression may shed light on pathway interactions. Smoc1 (SPARC-related modular calcium binding 1) is an extracellular calcium-binding matrix protein (Vannahme et al., 2002)(Okada et al., 2011)(Rainger et al., 2011). *Smoc1* expression was also upregulated up to 12-fold in a microarray screen for genes upregulated in Hedgehog-driven cerebellar tumors (Chiang, unpublished data), while *Smoc2* was not. However, *Smoc2* expression appears to be dependent on Hedgehog signaling in the testis and kidney (Pazin and Albrecht, 2009). As we have demonstrated in our current study, Hh regulates the expression of *Has2*, an essential enzyme for the production of hyaluronan, a major component of the ECM in some tissues. It remains to be determined if Hh signaling also regulates Smoc1 expression in basement membrane ECM. Smoc1 is also a Bmp antagonist (Rainger et al., 2011). As with Wnt, Hh and Bmp signalings often function concomitantly in the patterning of tissues, therefore investigating whether Hh modulates the expression of Smoc1, may reveal novel pathway interactions.

The role of *Has2* in joint development

We found that the regulation of *Has2* by Shh signaling is essential to digit joint patterning. In particular, loss of *Has2* induces ectopic joint formation via disruption of CSPGs. It is interesting to note that *Has2* expression seems to occur in two phases in the developing autopod; early Shh-induced *Has2* at E9.5-12 (this study) and a late-induced phase at around E14.5-E16.5, likely independent of Hh, in presumptive joints and perichondrium where Hh pathway is not activated (Dy et al., 2010). This late phase of

Has2 expression in the interzone coincides with the appearance of its cell surface receptor CD44 accumulation and the onset of joint morphogenesis including synovial joint formation (Craig et al., 1990; Edwards et al., 1994; Pitsillides et al., 1995). It has been proposed that HA plays an important role in synovial joint cavity formation through disruption of tissue integrity in the interzone, permitting separation of two opposing non-adherent surfaces (Lamb et al., 2003; Pacifici et al., 2005). The experimental support for this model comes from previous observation that exogenous application of HA-oligosaccharides to chick embryos led to displacement of endogenous HA and inhibition of joint cavitation (Dowthwaite et al., 1998). Our genetic study, however, suggests that HA is not required for cavitation as the loss of *Has2* function did not prevent cavity formation. Therefore, *Has2* or HA in the interzone is likely involved in other aspects of joint development such as articular cartilage formation or fluidity/hydration of the synovial cavity. Unfortunately, detailed analysis of digit joints in *Hoxb6-cre;Has2*$^{fl/-}$ mutants is not feasible due to severe joint patterning and chondrogenic defects. To circumvent this problem, I plan to use interzone specific Cre, such as *Gdf5-Cre*, to specifically abolish *Has2* function in the joint region. The results from this study will likely shed light on the mechanism of HA function in joint formation.

The contribution of paracrine Shh signaling in limb patterning

Shh morphogen, secreted from the ZPA, acts not only upon immediate neighboring cells to induce juxtacrine signaling but also over long distance (10 or more cells) to induce paracrine signaling during limb patterning. Fate mapping studies have shown that Shh-expressing cells and their descendents contribute to digits 4 and 5, and the posterior half

of digit 3, indicating that progenitors of digits 4, 5 and some of digit 3 may be influenced by juxtacrine signaling (Harfe et al., 2004). Interestingly, Shh signaling responsive genes, such as *Gli1* and *Ptch1*, are both downregulated near the ZPA after E10.5 (Ahn and Joyner, 2004), raising an intriguing question as to whether specification of digit 5 requires duration of Shh activity. Similar fate mapping studies, using *Gli1-Cre* to trace Shh-responsive cells and their descendents, have concluded that digits 2-5 are derived from progenitors receiving Shh signal (Ahn and Joyner, 2004), suggesting that the anterior digits, at least digit 2, are influenced by paracrine Shh signaling. Although these observations reveal the dynamic movement and contribution of expanding ZPA progenitor cells, the relative contribution of juxtacrine and paracrine Shh signaling in A-P patterning of the limb remain to be determined.

The twelve-pass transmembrane protein Dispatched (Disp) appears to be required for the release of lipidated Hh from its source for paracrine signaling (Burke et al., 1999; Caspary et al., 2002; Kawakami et al., 2002; Ma et al., 2002). In the absence of Disp, *Drosophila* Hh accumulated in the posterior compartment of the imaginal disc, where it is normally expressed, hence restricting long distance distribution of Hh protein across the boundary to the anterior compartment (Burke et al., 1999). In the mouse, there are two Disp homolog proteins. It is only Disp1, but not Disp2, that can rescue Disp function in *Drosophila* (Ma et al., 2002). Deletion of Disp1 disrupts Hedgehog paracrine signaling and results in only short-range juxtacrine signaling. However, *Disp1*-deficient mouse embryos die around E9.5 due to defective yolk sac angiogenesis (Caspary et al., 2002; Kawakami et al., 2002; Ma et al., 2002).

To address the precise contribution of juxtacrine and paracrine Shh signaling effects on limb patterning, it is necessary to conditionally and completely remove *Disp1* function in the early limb bud. I generated the *Disp1* conditional allele by inserting two LoxP sites flanking exon10 (Fig. 3.3A). Exon10 encodes 3/4 of the amino acids in the full-length mDisp1 protein and contains 11 of the 12 transmembrane domains. Deleting exon10 abolishes Disp1 function in the *Disp1-/-* null mutant. To generate the targeting construct, a ~12kb fragment, including a 4kb 5'- homologous arm, 4.2kb exon10 and 3.8kb 3'-homologous arm, was retrieved from the *Disp1* Bac clone. The first LoxP sequence was inserted into an Xba1 site 740bp upstream of exon10. The second LoxP sequence accompanied with a positive selection *frt-neo-frt* cassette was inserted into a BglII site 130bp downstream of exon10. Screening for positive mouse embryonic stem (ES) cell clones was carried out by both Southern blotting and PCR (Fig. 3.3B, Fig. 3.3C). The targeted clones were injected into blastocysts by the Vanderbilt Transgenic Core. Male chimeras were obtained and crossed to Black Swiss breeding females. Agouti pups were collected as heterozygotes carrying the $Disp1^{fl}$ allele. I generated *Disp1cko* mutants by crossing $Disp1^{fl/+}$ with *Hoxb6-Cre;* $Disp1^{+/fl}$.

The skeletal preparation of newborn *Disp1cko* hindlimbs showed a severe patterning phenotype with only 3 digits, indicating Disp1-mediated paracrine signaling is essential to digit patterning (Fig. 3.4). To better understand the role of paracrine Shh signaling to each digit, it is necessary to assign identities to those digits. To date, the ossification pattern of the tarsal bone and its connection with each digit is the major criterion for

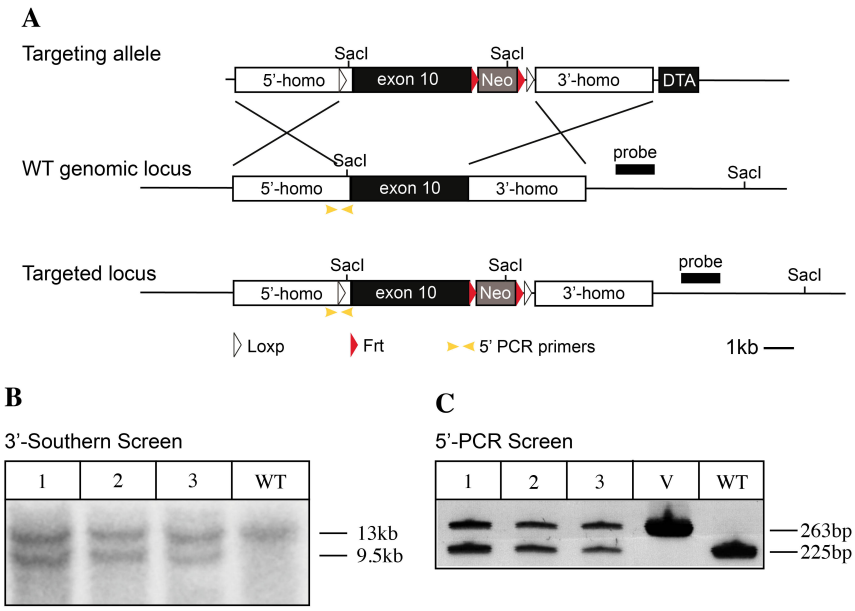

Figure 3.3. Generating the *Disp1* conditional knockout allele *Disp1*^{fl}.

(A) Illustration of *Disp1* conditional knockout targeting construct with two LoxP sequences flanking exon10, which encode 2/3 of Disp1 protein. A *frt-neo-frt* cassette was also inserted for positive selection. PGK driven diphthera toxin (DTA) was incorporated into the targeting vector to increase the efficiency of homologous recombination in ES cells. The location of DNA probe is indicated by thick black bar situated outside of 3' homologous arm whereas yellow arrowheads represents the location of PCR primers for 5'-screen. (B) Southern blotting was initially used to screen homologous events using the DNA probe. Genomic DNA was digested with SacI and the correct targeted locus (+) is represented by the 13 kb fragment whereas the non-targeted locus (-) shows 9.5 kb on the Southern blot. (C) PCR was subsequently used to confirm homologous event at 5' end of *Disp1* locus. The location of the primers are designed such that targeted locus will be amplified as a 263 bp fragment, whereas non-targeted locus will be amplified as a 225 bp fragment. Primers for PCR are forward: 5'-CACACCGACTCAATGCTGTGAAG -3' and reverse: 5'-CAGAATGGCGATGTAATTCCCC-3'.

assigning digit identity. However, the organization of metatarsal elements in our *Disp1cko* mutant limbs was also disrupted, which makes it difficult to determine the digit identities (Fig. 3.4). Alternatively, *Noggin*^{lacZ} knock-in allele provides a sensitive tool to detect early condensation events during digit formation, which will help define digit identities. Future analysis will be focused on characterizing digit phenotypes using this genetic tool. Moreover, I will confirm Shh distribution by immunostaining and assess Shh pathway activity by examining dedicated readouts such as *Gli1* and *Ptch1* by RNA *in situ* hybridization, as well as Shh signaling-dependent genes, such as *Gremlin, Hip1, Fgf4,* and *Hoxd13* in the posterior limb mesoderm or AER. Studies in this direction will help us understand the intrinsic properties of the Shh signaling cascade, and further dissect its roles in limb patterning.

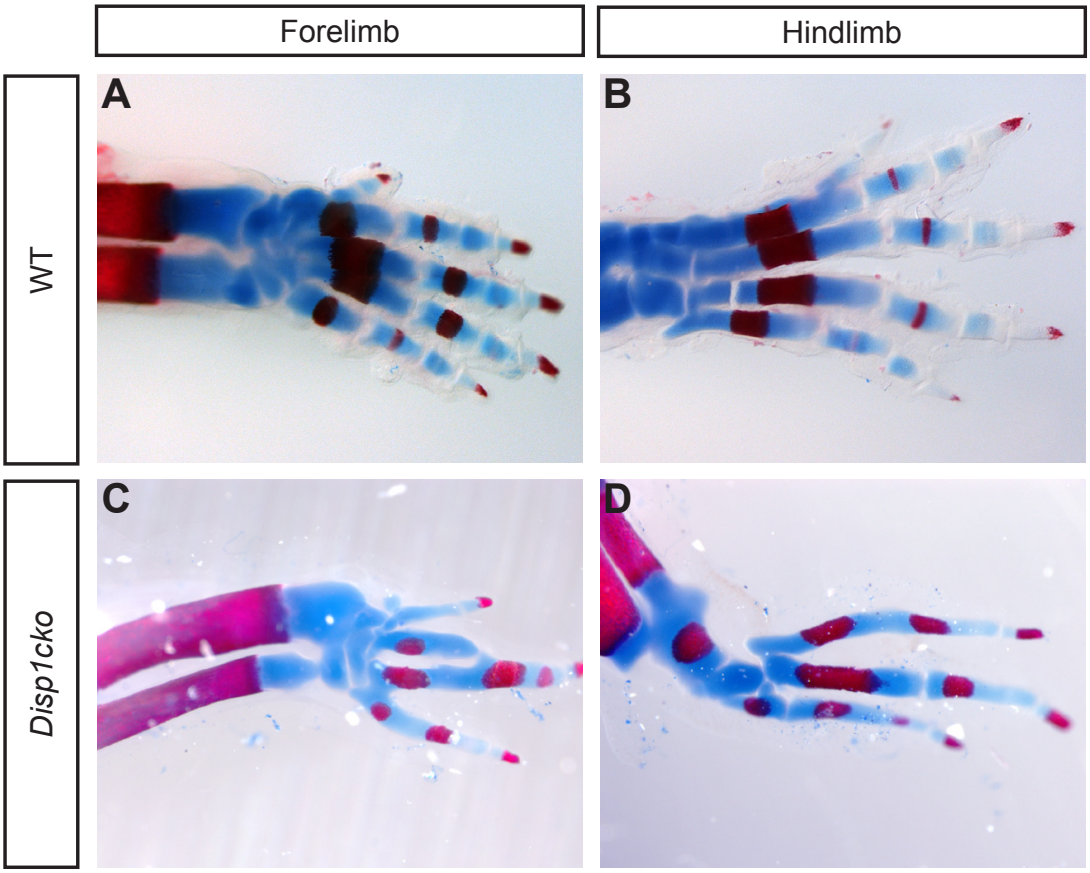

Figure 3.4. Loss of anterior digits in *Disp1cko* mutant hindlimbs.

Whole-mount skeletal elements of P0 wild-type (A,B) and *Disp1*^{cko} (C,D) forelimbs (A,C) and hindlimbs (B,D) stained with Alizarin red and Alcian blue. Severe digit loss are apparent in P0 *Disp1*^{cko} digits; note that there is only four digits in mutant forelimb (C) and three digits in mutant hindlimb (D). The digit identities in the mutant limbs require further characterization.

BIBLIOGRAPHY

Adamia, S., Maxwell, C.A., and Pilarski, L.M. (2005). Hyaluronan and hyaluronan synthases: potential therapeutic targets in cancer. Curr Drug Targets Cardiovasc Haematol Disord *5*, 3-14.

Ahn, S., and Joyner, A.L. (2004). Dynamic changes in the response of cells to positive hedgehog signaling during mouse limb patterning. Cell *118*, 505-516.

Ahrens, P.B., Solursh, M., and Reiter, R.S. (1977). Stage-related capacity for limb chondrogenesis in cell culture. Dev Biol *60*, 69-82.

Alison, M.R., Lin, W.R., Lim, S.M., and Nicholson, L.J. (2012). Cancer stem cells: in the line of fire. Cancer treatment reviews *38*, 589-598.

Amarilio, R., Viukov, S.V., Sharir, A., Eshkar-Oren, I., Johnson, R.S., and Zelzer, E. (2007). HIF1alpha regulation of Sox9 is necessary to maintain differentiation of hypoxic prechondrogenic cells during early skeletogenesis. Development *134*, 3917-3928.

Andersen, H. (1961). Histochemical studies on the histogenesis of the knee joint and superior tibio-fibular joint in human foetuses. Acta Anat (Basel) *46*, 279-303.

Bai, C.B., Stephen, D., and Joyner, A.L. (2004). All mouse ventral spinal cord patterning by hedgehog is Gli dependent and involves an activator function of Gli3. Dev Cell *6*, 103-115.

Bambakidis, N.C., and Onwuzulike, K. (2012). Sonic Hedgehog signaling and potential therapeutic indications. Vitamins and hormones *88*, 379-394.

Basson, C.T., Bachinsky, D.R., Lin, R.C., Levi, T., Elkins, J.A., Soults, J., Grayzel, D., Kroumpouzou, E., Traill, T.A., Leblanc-Straceski, J., *et al.* (1997). Mutations in human TBX5 [corrected] cause limb and cardiac malformation in Holt-Oram syndrome. Nat Genet *15*, 30-35.

Bastow, E.R., Lamb, K.J., Lewthwaite, J.C., Osborne, A.C., Kavanagh, E., Wheeler-Jones, C.P., and Pitsillides, A.A. (2005). Selective activation of the MEK-ERK pathway is regulated by mechanical stimuli in forming joints and promotes pericellular matrix formation. J Biol Chem *280*, 11749-11758.

Beachy, P.A., Karhadkar, S.S., and Berman, D.M. (2004). Tissue repair and stem cell renewal in carcinogenesis. Nature *432*, 324-331.

Bernert, B., Porsch, H., and Heldin, P. (2011). Hyaluronan synthase 2 (HAS2) promotes breast cancer cell invasion by suppression of tissue metalloproteinase inhibitor 1 (TIMP-1). J Biol Chem *286*, 42349-42359.

Bharadwaj, A.G., Kovar, J.L., Loughman, E., Elowsky, C., Oakley, G.G., and Simpson, M.A. (2009). Spontaneous metastasis of prostate cancer is promoted by excess hyaluronan synthesis and processing. Am J Pathol *174*, 1027-1036.

Bourguignon, L.Y. (2008). Hyaluronan-mediated CD44 activation of RhoGTPase signaling and cytoskeleton function promotes tumor progression. Semin Cancer Biol *18*, 251-259.

Bowers, M., Eng, L., Lao, Z., Turnbull, R.K., Bao, X., Riedel, E., Mackem, S., and Joyner, A.L. (2012). Limb anterior-posterior polarity integrates activator and repressor functions of GLI2 as well as GLI3. Dev Biol.

Burke, R., Nellen, D., Bellotto, M., Hafen, E., Senti, K.A., Dickson, B.J., and Basler, K. (1999). Dispatched, a novel sterol-sensing domain protein dedicated to the release of cholesterol-modified hedgehog from signaling cells. Cell *99*, 803-815.

Camenisch, T.D., Spicer, A.P., Brehm-Gibson, T., Biesterfeldt, J., Augustine, M.L., Calabro, A., Jr., Kubalak, S., Klewer, S.E., and McDonald, J.A. (2000). Disruption of hyaluronan synthase-2 abrogates normal cardiac morphogenesis and hyaluronan-mediated transformation of epithelium to mesenchyme. J Clin Invest *106*, 349-360.

Cash, D.E., Bock, C.B., Schughart, K., Linney, E., and Underhill, T.M. (1997). Retinoic acid receptor alpha function in vertebrate limb skeletogenesis: a modulator of chondrogenesis. J Cell Biol *136*, 445-457.

Caspary, T., Garcia-Garcia, M.J., Huangfu, D., Eggenschwiler, J.T., Wyler, M.R., Rakeman, A.S., Alcorn, H.L., and Anderson, K.V. (2002). Mouse Dispatched homolog1 is required for long-range, but not juxtacrine, Hh signaling. Curr Biol *12*, 1628-1632.

Chang, D.T., Lopez, A., von Kessler, D.P., Chiang, C., Simandl, B.K., Zhao, R., Seldin, M.F., Fallon, J.F., and Beachy, P.A. (1994). Products, genetic linkage and limb patterning activity of a murine hedgehog gene. Development *120*, 3339-3353.

Chiang, C., Litingtung, Y., Harris, M.P., Simandl, B.K., Li, Y., Beachy, P.A., and Fallon, J.F. (2001). Manifestation of the limb prepattern: limb development in the absence of sonic hedgehog function. Dev Biol *236*, 421-435.

Chiang, C., Litingtung, Y., Lee, E., Young, K.E., Corden, J.L., Westphal, H., and Beachy, P.A. (1996). Cyclopia and defective axial patterning in mice lacking Sonic hedgehog gene function. Nature *383*, 407-413.

Copeland, N.G., Jenkins, N.A., and Court, D.L. (2001). Recombineering: a powerful new tool for mouse functional genomics. Nat Rev Genet *2*, 769-779.

Craig, F.M., Bayliss, M.T., Bentley, G., and Archer, C.W. (1990). A role for hyaluronan in joint development. J Anat *171*, 17-23.

Crossley, P.H., Minowada, G., MacArthur, C.A., and Martin, G.R. (1996). Roles for FGF8 in the induction, initiation, and maintenance of chick limb development. Cell *84*, 127-136.

Dai, Y.S., and Cserjesi, P. (2002). The basic helix-loop-helix factor, HAND2, functions as a transcriptional activator by binding to E-boxes as a heterodimer. J Biol Chem *277*, 12604-12612.

Day, A.J. (1999). The structure and regulation of hyaluronan-binding proteins. Biochem Soc Trans *27*, 115-121.

Day, A.J., and Prestwich, G.D. (2002). Hyaluronan-binding proteins: tying up the giant. J Biol Chem *277*, 4585-4588.

Dowthwaite, G.P., Edwards, J.C., and Pitsillides, A.A. (1998). An essential role for the interaction between hyaluronan and hyaluronan binding proteins during joint development. The journal of histochemistry and cytochemistry : official journal of the Histochemistry Society *46*, 641-651.

Dudley, A.T., Ros, M.A., and Tabin, C.J. (2002). A re-examination of proximodistal patterning during vertebrate limb development. Nature *418*, 539-544.

Dy, P., Smits, P., Silvester, A., Penzo-Mendez, A., Dumitriu, B., Han, Y., de la Motte, C.A., Kingsley, D.M., and Lefebvre, V. (2010). Synovial joint morphogenesis requires the chondrogenic action of Sox5 and Sox6 in growth plate and articular cartilage. Dev Biol *341*, 346-359.

Eames, B.F., de la Fuente, L., and Helms, J.A. (2003). Molecular ontogeny of the skeleton. Birth Defects Res C Embryo Today *69*, 93-101.

Edwards, J.C., Wilkinson, L.S., Jones, H.M., Soothill, P., Henderson, K.J., Worrall, J.G., and Pitsillides, A.A. (1994). The formation of human synovial joint cavities: a possible role for hyaluronan and CD44 in altered interzone cohesion. J Anat *185 (Pt 2)*, 355-367.

Fernandez-Teran, M.A., Hinchliffe, J.R., and Ros, M.A. (2006). Birth and death of cells in limb development: a mapping study. Dev Dyn *235*, 2521-2537.

Firulli, B.A., Krawchuk, D., Centonze, V.E., Vargesson, N., Virshup, D.M., Conway, S.J., Cserjesi, P., Laufer, E., and Firulli, A.B. (2005). Altered Twist1 and Hand2 dimerization is associated with Saethre-Chotzen syndrome and limb abnormalities. Nat Genet *37*, 373-381.

Francis-West, P.H., Abdelfattah, A., Chen, P., Allen, C., Parish, J., Ladher, R., Allen, S., MacPherson, S., Luyten, F.P., and Archer, C.W. (1999a). Mechanisms of GDF-5 action during skeletal development. Development *126*, 1305-1315.

Francis-West, P.H., Parish, J., Lee, K., and Archer, C.W. (1999b). BMP/GDF-signalling interactions during synovial joint development. Cell and tissue research *296*, 111-119.

Galli, A., Robay, D., Osterwalder, M., Bao, X., Benazet, J.D., Tariq, M., Paro, R., Mackem, S., and Zeller, R. (2010). Distinct roles of Hand2 in initiating polarity and posterior Shh expression during the onset of mouse limb bud development. PLoS genetics *6*, e1000901.

Gavin, B.J., McMahon, J.A., and McMahon, A.P. (1990). Expression of multiple novel Wnt-1/int-1-related genes during fetal and adult mouse development. Genes Dev *4*, 2319-2332.

Gepstein, A., Shapiro, S., Arbel, G., Lahat, N., and Livne, E. (2002). Expression of matrix metalloproteinases in articular cartilage of temporomandibular and knee joints of mice during growth, maturation, and aging. Arthritis and rheumatism *46*, 3240-3250.

Gibson-Brown, J.J., Agulnik, S.I., Chapman, D.L., Alexiou, M., Garvey, N., Silver, L.M., and Papaioannou, V.E. (1996). Evidence of a role for T-box genes in the evolution of limb morphogenesis and the specification of forelimb/hindlimb identity. Mech Dev *56*, 93-101.

Goldring, M.B., Tsuchimochi, K., and Ijiri, K. (2006). The control of chondrogenesis. Journal of cellular biochemistry *97*, 33-44.

Goodrich, L.V., Milenkovic, L., Higgins, K.M., and Scott, M.P. (1997). Altered neural cell fates and medulloblastoma in mouse patched mutants. Science *277*, 1109-1113.

Hall, B.K., and Miyake, T. (1995). Divide, accumulate, differentiate: cell condensation in skeletal development revisited. The International journal of developmental biology *39*, 881-893.

Hallikas, O., Palin, K., Sinjushina, N., Rautiainen, R., Partanen, J., Ukkonen, E., and Taipale, J. (2006). Genome-wide prediction of mammalian enhancers based on analysis of transcription-factor binding affinity. Cell *124*, 47-59.

Hammerschmidt, M., Brook, A., and McMahon, A.P. (1997). The world according to hedgehog. Trends Genet *13*, 14-21.

Hardingham, T.E. (1979). The role of link-protein in the structure of cartilage proteoglycan aggregates. Biochem J *177*, 237-247.

Hardingham, T.E., and Fosang, A.J. (1992). Proteoglycans: many forms and many functions. FASEB J *6*, 861-870.

Harfe, B.D., Scherz, P.J., Nissim, S., Tian, H., McMahon, A.P., and Tabin, C.J. (2004). Evidence for an expansion-based temporal Shh gradient in specifying vertebrate digit identities. Cell *118*, 517-528.

Hartmann, C., and Tabin, C.J. (2000). Dual roles of Wnt signaling during chondrogenesis in the chicken limb. Development *127*, 3141-3159.

Hartmann, C., and Tabin, C.J. (2001). Wnt-14 plays a pivotal role in inducing synovial joint formation in the developing appendicular skeleton. Cell *104*, 341-351.

Hascall, V.C., Oegema, T.R., and Brown, M. (1976). Isolation and characterization of proteoglycans from chick limb bud chondrocytes grown in vitro. J Biol Chem *251*, 3511-3519.

Hill, R.E. (2007). How to make a zone of polarizing activity: insights into limb development via the abnormality preaxial polydactyly. Development, growth & differentiation *49*, 439-448.

Hill, R.E., Heaney, S.J., and Lettice, L.A. (2003). Sonic hedgehog: restricted expression and limb dysmorphologies. J Anat *202*, 13-20.

Hiraoka, S., Furuichi, T., Nishimura, G., Shibata, S., Yanagishita, M., Rimoin, D.L., Superti-Furga, A., Nikkels, P.G., Ogawa, M., Katsuyama, K., *et al.* (2007). Nucleotide-sugar transporter SLC35D1 is critical to chondroitin sulfate synthesis in cartilage and skeletal development in mouse and human. Nat Med *13*, 1363-1367.

Huang, X., Liu, J., Ketova, T., Fleming, J.T., Grover, V.K., Cooper, M.K., Litingtung, Y., and Chiang, C. (2010). Transventricular delivery of Sonic hedgehog is essential to cerebellar ventricular zone development. Proc Natl Acad Sci U S A *107*, 8422-8427.

Ingham, P.W. (1998a). The patched gene in development and cancer. Curr Opin Genet Dev *8*, 88-94.

Ingham, P.W. (1998b). Transducing Hedgehog: the story so far. EMBO J *17*, 3505-3511.

Ingham, P.W., and McMahon, A.P. (2001). Hedgehog signaling in animal development: paradigms and principles. Genes Dev *15*, 3059-3087.

James, C.G., Appleton, C.T., Ulici, V., Underhill, T.M., and Beier, F. (2005). Microarray analyses of gene expression during chondrocyte differentiation identifies novel regulators of hypertrophy. Mol Biol Cell *16*, 5316-5333.

Jiang, D., Liang, J., and Noble, P.W. (2007). Hyaluronan in tissue injury and repair. Annu Rev Cell Dev Biol *23*, 435-461.

Jiang, D., Liang, J., and Noble, P.W. (2011). Hyaluronan as an immune regulator in human diseases. Physiol Rev *91*, 221-264.

Jiang, J., and Hui, C.C. (2008). Hedgehog signaling in development and cancer. Dev Cell *15*, 801-812.

Kar, S., Deb, M., Sengupta, D., Shilpi, A., Bhutia, S.K., and Patra, S.K. (2012). Intricacies of hedgehog signaling pathways: a perspective in tumorigenesis. Experimental cell research *318*, 1959-1972.

Karsenty, G., and Wagner, E.F. (2002). Reaching a genetic and molecular understanding of skeletal development. Dev Cell *2*, 389-406.

Kavanagh, E., Abiri, M., Bland, Y.S., and Ashhurst, D.E. (2002). Division and death of cells in developing synovial joints and long bones. Cell biology international *26*, 679-688.

Kawakami, T., Kawcak, T., Li, Y.J., Zhang, W., Hu, Y., and Chuang, P.T. (2002). Mouse dispatched mutants fail to distribute hedgehog proteins and are defective in hedgehog signaling. Development *129*, 5753-5765.

Khan, I.M., Redman, S.N., Williams, R., Dowthwaite, G.P., Oldfield, S.F., and Archer, C.W. (2007). The development of synovial joints. Curr Top Dev Biol *79*, 1-36.

Kimura, S., and Shiota, K. (1996). Sequential changes of programmed cell death in developing fetal mouse limbs and its possible roles in limb morphogenesis. Journal of morphology *229*, 337-346.

Kinzler, K.W., and Vogelstein, B. (1990). The GLI gene encodes a nuclear protein which binds specific sequences in the human genome. Mol Cell Biol *10*, 634-642.

Klingensmith, J., Ang, S.L., Bachiller, D., and Rossant, J. (1999). Neural induction and patterning in the mouse in the absence of the node and its derivatives. Dev Biol *216*, 535-549.

Knudson, C.B. (1993). Hyaluronan receptor-directed assembly of chondrocyte pericellular matrix. J Cell Biol *120*, 825-834.

Knudson, C.B., Nofal, G.A., Pamintuan, L., and Aguiar, D.J. (1999). The chondrocyte pericellular matrix: a model for hyaluronan-mediated cell-matrix interactions. Biochem Soc Trans *27*, 142-147.

Knudson, C.B., and Toole, B.P. (1985). Changes in the pericellular matrix during differentiation of limb bud mesoderm. Dev Biol *112*, 308-318.

Knudson, C.B., and Toole, B.P. (1988). Epithelial-mesenchymal interaction in the regulation of hyaluronate production during limb development. Biochem Int *17*, 735-745.

Kobayashi, N., Miyoshi, S., Mikami, T., Koyama, H., Kitazawa, M., Takeoka, M., Sano, K., Amano, J., Isogai, Z., Niida, S., *et al.* (2010). Hyaluronan deficiency in tumor stroma impairs macrophage trafficking and tumor neovascularization. Cancer Res *70*, 7073-7083.

Kochhar, D.M., Penner, J.D., and Hickey, T. (1984). Retinoic acid enhances the displacement of newly synthesized hyaluronate from cell layer to culture medium during early phases of chondrogenesis. Cell Differ *14*, 213-221.

Kohda, D., Morton, C.J., Parkar, A.A., Hatanaka, H., Inagaki, F.M., Campbell, I.D., and Day, A.J. (1996). Solution structure of the link module: a hyaluronan-binding domain involved in extracellular matrix stability and cell migration. Cell *86*, 767-775.

Kosaki, R., Watanabe, K., and Yamaguchi, Y. (1999). Overproduction of hyaluronan by expression of the hyaluronan synthase Has2 enhances anchorage-independent growth and tumorigenicity. Cancer Res *59*, 1141-1145.

Kosher, R.A., and Savage, M.P. (1981). Glycosaminoglycan synthesis by the apical ectodermal ridge of chick limb bud. Nature *291*, 231-232.

Kosher, R.A., Savage, M.P., and Walker, K.H. (1981). A gradation of hyaluronate accumulation along the proximodistal axis of the embryonic chick limb bud. J Embryol Exp Morphol *63*, 85-98.

Koyama, E., Shibukawa, Y., Nagayama, M., Sugito, H., Young, B., Yuasa, T., Okabe, T., Ochiai, T., Kamiya, N., Rountree, R.B., *et al.* (2008). A distinct cohort of progenitor cells participates in synovial joint and articular cartilage formation during mouse limb skeletogenesis. Dev Biol *316*, 62-73.

Kramer, M.W., Escudero, D.O., Lokeshwar, S.D., Golshani, R., Ekwenna, O.O., Acosta, K., Merseburger, A.S., Soloway, M., and Lokeshwar, V.B. (2011). Association of hyaluronic acid family members (HAS1, HAS2, and HYAL-1) with bladder cancer diagnosis and prognosis. Cancer *117*, 1197-1209.

Kraus, P., Fraidenraich, D., and Loomis, C.A. (2001). Some distal limb structures develop in mice lacking Sonic hedgehog signaling. Mech Dev *100*, 45-58.

Kulyk, W.M., and Kosher, R.A. (1987). Temporal and spatial analysis of hyaluronidase activity during development of the embryonic chick limb bud. Dev Biol *120*, 535-541.

Lamb, K.J., Lewthwaite, J.C., Bastow, E.R., and Pitsillides, A.A. (2003). Defining boundaries during joint cavity formation: going out on a limb. International journal of experimental pathology *84*, 55-67.

Lee, G.M., Johnstone, B., Jacobson, K., and Caterson, B. (1993). The dynamic structure of the pericellular matrix on living cells. J Cell Biol *123*, 1899-1907.

Lee, J.J., Ekker, S.C., von Kessler, D.P., Porter, J.A., Sun, B.I., and Beachy, P.A. (1994). Autoproteolysis in hedgehog protein biogenesis. Science *266*, 1528-1537.
Lee, J.Y., and Spicer, A.P. (2000). Hyaluronan: a multifunctional, megaDalton, stealth molecule. Curr Opin Cell Biol *12*, 581-586.

Lefebvre, V., Li, P., and de Crombrugghe, B. (1998). A new long form of Sox5 (L-Sox5), Sox6 and Sox9 are coexpressed in chondrogenesis and cooperatively activate the type II collagen gene. EMBO J *17*, 5718-5733.

Lettice, L.A., Heaney, S.J., Purdie, L.A., Li, L., de Beer, P., Oostra, B.A., Goode, D., Elgar, G., Hill, R.E., and de Graaff, E. (2003). A long-range Shh enhancer regulates expression in the developing limb and fin and is associated with preaxial polydactyly. Hum Mol Genet *12*, 1725-1735.

Lev, R., and Spicer, S.S. (1964). Specific Staining of Sulphate Groups with Alcian Blue at Low Ph. J Histochem Cytochem *12*, 309.

Lewis, P.M., Dunn, M.P., McMahon, J.A., Logan, M., Martin, J.F., St-Jacques, B., and McMahon, A.P. (2001). Cholesterol modification of sonic hedgehog is required for long-range signaling activity and effective modulation of signaling by Ptc1. Cell *105*, 599-612.

Li, C., Xu, X., Nelson, D.K., Williams, T., Kuehn, M.R., and Deng, C.X. (2005). FGFR1 function at the earliest stages of mouse limb development plays an indispensable role in subsequent autopod morphogenesis. Development *132*, 4755-4764.

Li, Q.Y., Newbury-Ecob, R.A., Terrett, J.A., Wilson, D.I., Curtis, A.R., Yi, C.H., Gebuhr, T., Bullen, P.J., Robson, S.C., Strachan, T., *et al.* (1997). Holt-Oram syndrome is caused by mutations in TBX5, a member of the Brachyury (T) gene family. Nat Genet *15*, 21-29.

Li, Y., Gordon, J., Manley, N.R., Litingtung, Y., and Chiang, C. (2008). Bmp4 is required for tracheal formation: a novel mouse model for tracheal agenesis. Dev Biol *322*, 145-155.

Li, Y., and Heldin, P. (2001). Hyaluronan production increases the malignant properties of mesothelioma cells. Br J Cancer *85*, 600-607.

Li, Y., Li, L., Brown, T.J., and Heldin, P. (2007a). Silencing of hyaluronan synthase 2 suppresses the malignant phenotype of invasive breast cancer cells. Int J Cancer *120*, 2557-2567.

Li, Y., Toole, B.P., Dealy, C.N., and Kosher, R.A. (2007b). Hyaluronan in limb morphogenesis. Dev Biol *305*, 411-420.

Li, Y., Zhang, H., Choi, S.C., Litingtung, Y., and Chiang, C. (2004). Sonic hedgehog signaling regulates Gli3 processing, mesenchymal proliferation, and differentiation during mouse lung organogenesis. Dev Biol *270*, 214-231.

Li, Y., Zhang, H., Litingtung, Y., and Chiang, C. (2006). Cholesterol modification restricts the spread of Shh gradient in the limb bud. Proc Natl Acad Sci U S A *103*, 6548-6553.

Litingtung, Y., Dahn, R.D., Li, Y., Fallon, J.F., and Chiang, C. (2002). Shh and Gli3 are dispensable for limb skeleton formation but regulate digit number and identity. Nature *418*, 979-983.

Liu, N., Barbosa, A.C., Chapman, S.L., Bezprozvannaya, S., Qi, X., Richardson, J.A., Yanagisawa, H., and Olson, E.N. (2009). DNA binding-dependent and -independent functions of the Hand2 transcription factor during mouse embryogenesis. Development *136*, 933-942.

Liu, P., Jenkins, N.A., and Copeland, N.G. (2003). A highly efficient recombineering-based method for generating conditional knockout mutations. Genome Res *13*, 476-484.

Logan, M., Martin, J.F., Nagy, A., Lobe, C., Olson, E.N., and Tabin, C.J. (2002). Expression of Cre Recombinase in the developing mouse limb bud driven by a Prxl enhancer. Genesis *33*, 77-80.

Lopez-Martinez, A., Chang, D.T., Chiang, C., Porter, J.A., Ros, M.A., Simandl, B.K., Beachy, P.A., and Fallon, J.F. (1995). Limb-patterning activity and restricted

posterior localization of the amino-terminal product of Sonic hedgehog cleavage. Curr Biol *5*, 791-796.

Lopez-Rios, J., Speziale, D., Robay, D., Scotti, M., Osterwalder, M., Nusspaumer, G., Galli, A., Hollander, G.A., Kmita, M., and Zeller, R. (2012). GLI3 constrains digit number by controlling both progenitor proliferation and BMP-dependent exit to chondrogenesis. Dev Cell *22*, 837-848.

Lowe, L.A., Yamada, S., and Kuehn, M.R. (2000). HoxB6-Cre transgenic mice express Cre recombinase in extra-embryonic mesoderm, in lateral plate and limb mesoderm and at the midbrain/hindbrain junction. Genesis *26*, 118-120.

Ma, Y., Erkner, A., Gong, R., Yao, S., Taipale, J., Basler, K., and Beachy, P.A. (2002). Hedgehog-mediated patterning of the mammalian embryo requires transporter-like function of dispatched. Cell *111*, 63-75.

Maleski, M.P., and Knudson, C.B. (1996a). Hyaluronan-mediated aggregation of limb bud mesenchyme and mesenchymal condensation during chondrogenesis. Exp Cell Res *225*, 55-66.

Maleski, M.P., and Knudson, C.B. (1996b). Matrix accumulation and retention in embryonic cartilage and in vitro chondrogenesis. Connect Tissue Res *34*, 75-86.

Marigo, V., Johnson, R.L., Vortkamp, A., and Tabin, C.J. (1996). Sonic hedgehog differentially regulates expression of GLI and GLI3 during limb development. Dev Biol *180*, 273-283.

Markus, M., and Benezra, R. (1999). Two isoforms of protein disulfide isomerase alter the dimerization status of E2A proteins by a redox mechanism. J Biol Chem *274*, 1040-1049.

Matsumoto, K., Li, Y., Jakuba, C., Sugiyama, Y., Sayo, T., Okuno, M., Dealy, C.N., Toole, B.P., Takeda, J., Yamaguchi, Y., *et al.* (2009). Conditional inactivation of Has2 reveals a crucial role for hyaluronan in skeletal growth, patterning, chondrocyte maturation and joint formation in the developing limb. Development *136*, 2825-2835.

McMahon, A.P., Ingham, P.W., and Tabin, C.J. (2003). Developmental roles and clinical significance of hedgehog signaling. Current topics in developmental biology *53*, 1-114.

McMahon, J.A., Takada, S., Zimmerman, L.B., Fan, C.M., Harland, R.M., and McMahon, A.P. (1998). Noggin-mediated antagonism of BMP signaling is required for growth and patterning of the neural tube and somite. Genes Dev *12*, 1438-1452.

Merida-Velasco, J.A., Sanchez-Montesinos, I., Espin-Ferra, J., Rodriguez-Vazquez, J.F., Merida-Velasco, J.R., and Jimenez-Collado, J. (1997). Development of the human knee joint. The Anatomical record *248*, 269-278.

Merino, R., Macias, D., Ganan, Y., Economides, A.N., Wang, X., Wu, Q., Stahl, N., Sampath, K.T., Varona, P., and Hurle, J.M. (1999). Expression and function of Gdf-5 during digit skeletogenesis in the embryonic chick leg bud. Dev Biol *206*, 33-45.

Mo, R., Freer, A.M., Zinyk, D.L., Crackower, M.A., Michaud, J., Heng, H.H., Chik, K.W., Shi, X.M., Tsui, L.C., Cheng, S.H., *et al.* (1997). Specific and redundant functions of Gli2 and Gli3 zinc finger genes in skeletal patterning and development. Development *124*, 113-123.

Mohanty-Hejmadi, P., Dutta, S.K., and Mahapatra, P. (1992). Limbs generated at site of tail amputation in marbled balloon frog after vitamin A treatment. Nature *355*, 352-353.

Morgelin, M., Heinegard, D., Engel, J., and Paulsson, M. (1994). The cartilage proteoglycan aggregate: assembly through combined protein-carbohydrate and protein-protein interactions. Biophys Chem *50*, 113-128.

Morgelin, M., Paulsson, M., Hardingham, T.E., Heinegard, D., and Engel, J. (1988). Cartilage proteoglycans. Assembly with hyaluronate and link protein as studied by electron microscopy. Biochem J *253*, 175-185.

Mori, C., Nakamura, N., Kimura, S., Irie, H., Takigawa, T., and Shiota, K. (1995). Programmed cell death in the interdigital tissue of the fetal mouse limb is apoptosis with DNA fragmentation. The Anatomical record *242*, 103-110.

Motoyama, J., Liu, J., Mo, R., Ding, Q., Post, M., and Hui, C.C. (1998). Essential function of Gli2 and Gli3 in the formation of lung, trachea and oesophagus. Nat Genet *20*, 54-57.

Motoyama, J., Milenkovic, L., Iwama, M., Shikata, Y., Scott, M.P., and Hui, C.C. (2003). Differential requirement for Gli2 and Gli3 in ventral neural cell fate specification. Dev Biol *259*, 150-161.

Munaim, S.I., Klagsbrun, M., and Toole, B.P. (1991). Hyaluronan-dependent pericellular coats of chick embryo limb mesodermal cells: induction by basic fibroblast growth factor. Dev Biol *143*, 297-302.

Murtaugh, L.C., Chyung, J.H., and Lassar, A.B. (1999). Sonic hedgehog promotes somitic chondrogenesis by altering the cellular response to BMP signaling. Genes Dev *13*, 225-237.

Nagy, A., Rossant, J., Nagy, R., Abramow-Newerly, W., and Roder, J.C. (1993). Derivation of completely cell culture-derived mice from early-passage embryonic stem cells. Proc Natl Acad Sci U S A *90*, 8424-8428.

Nakamura, K., Shirai, T., Morishita, S., Uchida, S., Saeki-Miura, K., and Makishima, F. (1999). p38 mitogen-activated protein kinase functionally contributes to chondrogenesis induced by growth/differentiation factor-5 in ATDC5 cells. Experimental cell research *250*, 351-363.

Nelson, C.E., Morgan, B.A., Burke, A.C., Laufer, E., DiMambro, E., Murtaugh, L.C., Gonzales, E., Tessarollo, L., Parada, L.F., and Tabin, C. (1996). Analysis of Hox gene expression in the chick limb bud. Development *122*, 1449-1466.

Ng, L.J., Wheatley, S., Muscat, G.E., Conway-Campbell, J., Bowles, J., Wright, E., Bell, D.M., Tam, P.P., Cheah, K.S., and Koopman, P. (1997). SOX9 binds DNA, activates transcription, and coexpresses with type II collagen during chondrogenesis in the mouse. Dev Biol *183*, 108-121.

Nieuwenhuis, E., and Hui, C.C. (2005). Hedgehog signaling and congenital malformations. Clinical genetics *67*, 193-208.

Nieuwenhuis, E., Motoyama, J., Barnfield, P.C., Yoshikawa, Y., Zhang, X., Mo, R., Crackower, M.A., and Hui, C.C. (2006). Mice with a targeted mutation of patched2 are viable but develop alopecia and epidermal hyperplasia. Mol Cell Biol *26*, 6609-6622.

Nishida, Y., Knudson, C.B., Nietfeld, J.J., Margulis, A., and Knudson, W. (1999). Antisense inhibition of hyaluronan synthase-2 in human articular chondrocytes inhibits proteoglycan retention and matrix assembly. J Biol Chem *274*, 21893-21899.

Niswander, L., Jeffrey, S., Martin, G.R., and Tickle, C. (1994). A positive feedback loop coordinates growth and patterning in the vertebrate limb. Nature *371*, 609-612.

Nusslein-Volhard, C., and Wieschaus, E. (1980). Mutations affecting segment number and polarity in Drosophila. Nature *287*, 795-801.

Oberlender, S.A., and Tuan, R.S. (1994). Spatiotemporal profile of N-cadherin expression in the developing limb mesenchyme. Cell adhesion and communication *2*, 521-537.

Ogura, T., Alvarez, I.S., Vogel, A., Rodriguez, C., Evans, R.M., and Izpisua Belmonte, J.C. (1996). Evidence that Shh cooperates with a retinoic acid inducible co-factor to establish ZPA-like activity. Development *122*, 537-542.

Okuda, H., Kobayashi, A., Xia, B., Watabe, M., Pai, S.K., Hirota, S., Xing, F., Liu, W., Pandey, P.R., Fukuda, K.*, et al.* (2012). Hyaluronan synthase HAS2 promotes

tumor progression in bone by stimulating the interaction of breast cancer stem-like cells with macrophages and stromal cells. Cancer Res *72*, 537-547.

Olsen, B.R., Reginato, A.M., and Wang, W. (2000). Bone development. Annual review of cell and developmental biology *16*, 191-220.

Osborne, A.C., Lamb, K.J., Lewthwaite, J.C., Dowthwaite, G.P., and Pitsillides, A.A. (2002). Short-term rigid and flaccid paralyses diminish growth of embryonic chick limbs and abrogate joint cavity formation but differentially preserve pre-cavitated joints. Journal of musculoskeletal & neuronal interactions *2*, 448-456.

Pacifici, M., Koyama, E., and Iwamoto, M. (2005). Mechanisms of synovial joint and articular cartilage formation: recent advances, but many lingering mysteries. Birth Defects Res C Embryo Today *75*, 237-248.

Pacifici, M., Koyama, E., Shibukawa, Y., Wu, C., Tamamura, Y., Enomoto-Iwamoto, M., and Iwamoto, M. (2006). Cellular and molecular mechanisms of synovial joint and articular cartilage formation. Ann N Y Acad Sci *1068*, 74-86.

Paiva, P., Van Damme, M.P., Tellbach, M., Jones, R.L., Jobling, T., and Salamonsen, L.A. (2005). Expression patterns of hyaluronan, hyaluronan synthases and hyaluronidases indicate a role for hyaluronan in the progression of endometrial cancer. Gynecol Oncol *98*, 193-202.

Pan, Y., Bai, C.B., Joyner, A.L., and Wang, B. (2006). Sonic hedgehog signaling regulates Gli2 transcriptional activity by suppressing its processing and degradation. Mol Cell Biol *26*, 3365-3377.

Park, H.L., Bai, C., Platt, K.A., Matise, M.P., Beeghly, A., Hui, C.C., Nakashima, M., and Joyner, A.L. (2000). Mouse Gli1 mutants are viable but have defects in SHH signaling in combination with a Gli2 mutation. Development *127*, 1593-1605.

Pitsillides, A.A. (2003). Identifying and characterizing the joint cavity-forming cell. Cell Biochem Funct *21*, 235-240.

Pitsillides, A.A., Archer, C.W., Prehm, P., Bayliss, M.T., and Edwards, J.C. (1995). Alterations in hyaluronan synthesis during developing joint cavitation. The journal of histochemistry and cytochemistry : official journal of the Histochemistry Society *43*, 263-273.

Pitsillides, A.A., and Ashhurst, D.E. (2008). A critical evaluation of specific aspects of joint development. Dev Dyn *237*, 2284-2294.

Platt, K.A., Michaud, J., and Joyner, A.L. (1997). Expression of the mouse Gli and Ptc genes is adjacent to embryonic sources of hedgehog signals suggesting a conservation of pathways between flies and mice. Mech Dev *62*, 121-135.

Porter, J.A., Ekker, S.C., Park, W.J., von Kessler, D.P., Young, K.E., Chen, C.H., Ma, Y., Woods, A.S., Cotter, R.J., Koonin, E.V.*, et al.* (1996a). Hedgehog patterning activity: role of a lipophilic modification mediated by the carboxy-terminal autoprocessing domain. Cell *86*, 21-34.

Porter, J.A., von Kessler, D.P., Ekker, S.C., Young, K.E., Lee, J.J., Moses, K., and Beachy, P.A. (1995). The product of hedgehog autoproteolytic cleavage active in local and long-range signalling. Nature *374*, 363-366.

Porter, J.A., Young, K.E., and Beachy, P.A. (1996b). Cholesterol modification of hedgehog signaling proteins in animal development. Science *274*, 255-259.

Provot, S., Zinyk, D., Gunes, Y., Kathri, R., Le, Q., Kronenberg, H.M., Johnson, R.S., Longaker, M.T., Giaccia, A.J., and Schipani, E. (2007). Hif-1alpha regulates differentiation of limb bud mesenchyme and joint development. J Cell Biol *177*, 451-464.

Read, T.A., Fogarty, M.P., Markant, S.L., McLendon, R.E., Wei, Z., Ellison, D.W., Febbo, P.G., and Wechsler-Reya, R.J. (2009). Identification of CD15 as a marker for tumor-propagating cells in a mouse model of medulloblastoma. Cancer Cell *15*, 135-147.

Riddle, R.D., Ensini, M., Nelson, C., Tsuchida, T., Jessell, T.M., and Tabin, C. (1995). Induction of the LIM homeobox gene Lmx1 by WNT7a establishes dorsoventral pattern in the vertebrate limb. Cell *83*, 631-640.

Riddle, R.D., Johnson, R.L., Laufer, E., and Tabin, C. (1993). Sonic hedgehog mediates the polarizing activity of the ZPA. Cell *75*, 1401-1416.

Rodriguez, C.I., Buchholz, F., Galloway, J., Sequerra, R., Kasper, J., Ayala, R., Stewart, A.F., and Dymecki, S.M. (2000). High-efficiency deleter mice show that FLPe is an alternative to Cre-loxP. Nat Genet *25*, 139-140.

Roessler, E., Belloni, E., Gaudenz, K., Jay, P., Berta, P., Scherer, S.W., Tsui, L.C., and Muenke, M. (1996). Mutations in the human Sonic Hedgehog gene cause holoprosencephaly. Nat Genet *14*, 357-360.

Rowe, D.A., Cairns, J.M., and Fallon, J.F. (1982). Spatial and temporal patterns of cell death in limb bud mesoderm after apical ectodermal ridge removal. Dev Biol *93*, 83-91.

Ryan, K.E., and Chiang, C. (2012). Hedgehog secretion and signal transduction in vertebrates. J Biol Chem *287*, 17905-17913.

Sagai, T., Hosoya, M., Mizushina, Y., Tamura, M., and Shiroishi, T. (2005). Elimination of a long-range cis-regulatory module causes complete loss of limb-specific Shh expression and truncation of the mouse limb. Development *132*, 797-803.

Scherz, P.J., McGlinn, E., Nissim, S., and Tabin, C.J. (2007). Extended exposure to Sonic hedgehog is required for patterning the posterior digits of the vertebrate limb. Dev Biol *308*, 343-354.

Seghatoleslami, M.R., Roman-Blas, J.A., Rainville, A.M., Modaressi, R., Danielson, K.G., and Tuan, R.S. (2003). Progression of chondrogenesis in C3H10T1/2 cells is associated with prolonged and tight regulation of ERK1/2. Journal of cellular biochemistry *88*, 1129-1144.

Seo, H.S., and Serra, R. (2007). Deletion of Tgfbr2 in Prx1-cre expressing mesenchyme results in defects in development of the long bones and joints. Dev Biol *310*, 304-316.

Seyfried, N.T., McVey, G.F., Almond, A., Mahoney, D.J., Dudhia, J., and Day, A.J. (2005). Expression and purification of functionally active hyaluronan-binding domains from human cartilage link protein, aggrecan and versican: formation of ternary complexes with defined hyaluronan oligosaccharides. J Biol Chem *280*, 5435-5448.

Shinomura, T., Kimata, K., Oike, Y., Maeda, N., Yano, S., and Suzuki, S. (1984). Appearance of distinct types of proteoglycan in a well-defined temporal and spatial pattern during early cartilage formation in the chick limb. Dev Biol *103*, 211-220.
Simpson, M.A. (2006). Concurrent expression of hyaluronan biosynthetic and processing enzymes promotes growth and vascularization of prostate tumors in mice. Am J Pathol *169*, 247-257.

Simpson, M.A., Reiland, J., Burger, S.R., Furcht, L.T., Spicer, A.P., Oegema, T.R., Jr., and McCarthy, J.B. (2001). Hyaluronan synthase elevation in metastatic prostate carcinoma cells correlates with hyaluronan surface retention, a prerequisite for rapid adhesion to bone marrow endothelial cells. J Biol Chem *276*, 17949-17957.

Simpson, M.A., Wilson, C.M., and McCarthy, J.B. (2002). Inhibition of prostate tumor cell hyaluronan synthesis impairs subcutaneous growth and vascularization in immunocompromised mice. Am J Pathol *161*, 849-857.

Sohaskey, M.L., Yu, J., Diaz, M.A., Plaas, A.H., and Harland, R.M. (2008). JAWS coordinates chondrogenesis and synovial joint positioning. Development *135*, 2215-2220.

Stanton, L.A., Sabari, S., Sampaio, A.V., Underhill, T.M., and Beier, F. (2004). p38 MAP kinase signalling is required for hypertrophic chondrocyte differentiation. Biochem J *378*, 53-62.

Storm, E.E., and Kingsley, D.M. (1996). Joint patterning defects caused by single and double mutations in members of the bone morphogenetic protein (BMP) family. Development *122*, 3969-3979.

Sun, X., Mariani, F.V., and Martin, G.R. (2002). Functions of FGF signalling from the apical ectodermal ridge in limb development. Nature *418*, 501-508.

Taipale, J., and Beachy, P.A. (2001). The Hedgehog and Wnt signalling pathways in cancer. Nature *411*, 349-354.

Taipale, J., Chen, J.K., Cooper, M.K., Wang, B., Mann, R.K., Milenkovic, L., Scott, M.P., and Beachy, P.A. (2000). Effects of oncogenic mutations in Smoothened and Patched can be reversed by cyclopamine. Nature *406*, 1005-1009.

Tavella, S., Biticchi, R., Morello, R., Castagnola, P., Musante, V., Costa, D., Cancedda, R., and Garofalo, S. (2006). Forced chondrocyte expression of sonic hedgehog impairs joint formation affecting proliferation and apoptosis. Matrix biology : journal of the International Society for Matrix Biology *25*, 389-397.

te Welscher, P., Zuniga, A., Kuijper, S., Drenth, T., Goedemans, H.J., Meijlink, F., and Zeller, R. (2002). Progression of vertebrate limb development through SHH-mediated counteraction of GLI3. Science *298*, 827-830.

Tien, J.Y., and Spicer, A.P. (2005). Three vertebrate hyaluronan synthases are expressed during mouse development in distinct spatial and temporal patterns. Dev Dyn *233*, 130-141.

Toole, B.P. (2004). Hyaluronan: from extracellular glue to pericellular cue. Nat Rev Cancer *4*, 528-539.

Toole, B.P., and Hascall, V.C. (2002). Hyaluronan and tumor growth. Am J Pathol *161*, 745-747.

Towers, M., Wolpert, L., and Tickle, C. Gradients of signalling in the developing limb. Curr Opin Cell Biol *24*, 181-187.

Towers, M., Wolpert, L., and Tickle, C. (2011). Gradients of signalling in the developing limb. Curr Opin Cell Biol *24*, 181-187.

Tsonis, P.A., and Walker, E. (1991). Cell populations synthesizing cartilage proteoglycan core protein in the early chick limb bud. Biochem Biophys Res Commun *174*, 688-695.

Turley, E.A., Noble, P.W., and Bourguignon, L.Y. (2002). Signaling properties of hyaluronan receptors. J Biol Chem *277*, 4589-4592.

Udabage, L., Brownlee, G.R., Waltham, M., Blick, T., Walker, E.C., Heldin, P., Nilsson, S.K., Thompson, E.W., and Brown, T.J. (2005). Antisense-mediated suppression of hyaluronan synthase 2 inhibits the tumorigenesis and progression of breast cancer. Cancer Res *65*, 6139-6150.

Vissers, L.E., Lausch, E., Unger, S., Campos-Xavier, A.B., Gilissen, C., Rossi, A., Del Rosario, M., Venselaar, H., Knoll, U., Nampoothiri, S.*, et al.* (2011). Chondrodysplasia and abnormal joint development associated with mutations in IMPAD1, encoding the Golgi-resident nucleotide phosphatase, gPAPP. Am J Hum Genet *88*, 608-615.

Vogel, A., Rodriguez, C., Warnken, W., and Izpisua Belmonte, J.C. (1995). Dorsal cell fate specified by chick Lmx1 during vertebrate limb development. Nature *378*, 716-720.

Vokes, S.A., Ji, H., McCuine, S., Tenzen, T., Giles, S., Zhong, S., Longabaugh, W.J., Davidson, E.H., Wong, W.H., and McMahon, A.P. (2007). Genomic characterization of Gli-activator targets in sonic hedgehog-mediated neural patterning. Development *134*, 1977-1989.

Vokes, S.A., Ji, H., Wong, W.H., and McMahon, A.P. (2008). A genome-scale analysis of the cis-regulatory circuitry underlying sonic hedgehog-mediated patterning of the mammalian limb. Genes Dev *22*, 2651-2663.

Vortkamp, A., Gessler, M., and Grzeschik, K.H. (1995). Identification of optimized target sequences for the GLI3 zinc finger protein. DNA Cell Biol *14*, 629-634.

Wang, B., Fallon, J.F., and Beachy, P.A. (2000). Hedgehog-regulated processing of Gli3 produces an anterior/posterior repressor gradient in the developing vertebrate limb. Cell *100*, 423-434.

Watanabe, H., and Yamada, Y. (1999). Mice lacking link protein develop dwarfism and craniofacial abnormalities. Nat Genet *21*, 225-229.

Weedon, M.N., Lango, H., Lindgren, C.M., Wallace, C., Evans, D.M., Mangino, M., Freathy, R.M., Perry, J.R., Stevens, S., Hall, A.S.*, et al.* (2008). Genome-wide association analysis identifies 20 loci that influence adult height. Nat Genet *40*, 575-583.

Wetmore, C. (2003). Sonic hedgehog in normal and neoplastic proliferation: insight gained from human tumors and animal models. Curr Opin Genet Dev *13*, 34-42.

Whatcott, C.J., Han, H., Posner, R.G., Hostetter, G., and Von Hoff, D.D. (2011). Targeting the tumor microenvironment in cancer: why hyaluronidase deserves a second look. Cancer Discov *1*, 291-296.

Wilson, D.G., Phamluong, K., Lin, W.Y., Barck, K., Carano, R.A., Diehl, L., Peterson, A.S., Martin, F., and Solloway, M.J. (2012). Chondroitin sulfate synthase 1 (Chsy1) is required for bone development and digit patterning. Dev Biol *363*, 413-425.

Yang, Y., Drossopoulou, G., Chuang, P.T., Duprez, D., Marti, E., Bumcrot, D., Vargesson, N., Clarke, J., Niswander, L., McMahon, A.*, et al.* (1997). Relationship between dose, distance and time in Sonic Hedgehog-mediated regulation of anteroposterior polarity in the chick limb. Development *124*, 4393-4404.

Yoon, B.S., Ovchinnikov, D.A., Yoshii, I., Mishina, Y., Behringer, R.R., and Lyons, K.M. (2005). Bmpr1a and Bmpr1b have overlapping functions and are essential for chondrogenesis in vivo. Proc Natl Acad Sci U S A *102*, 5062-5067.

Yu, K., and Ornitz, D.M. (2008). FGF signaling regulates mesenchymal differentiation and skeletal patterning along the limb bud proximodistal axis. Development *135*, 483-491.

Zhao, C., Chen, A., Jamieson, C.H., Fereshteh, M., Abrahamsson, A., Blum, J., Kwon, H.Y., Kim, J., Chute, J.P., Rizzieri, D.*, et al.* (2009). Hedgehog signalling is essential for maintenance of cancer stem cells in myeloid leukaemia. Nature *458*, 776-779.

Zhu, J., Nakamura, E., Nguyen, M.T., Bao, X., Akiyama, H., and Mackem, S. (2008). Uncoupling Sonic hedgehog control of pattern and expansion of the developing limb bud. Dev Cell *14*, 624-632.

Zoltan-Jones, A., Huang, L., Ghatak, S., and Toole, B.P. (2003). Elevated hyaluronan production induces mesenchymal and transformed properties in epithelial cells. J Biol Chem *278*, 45801-45810.

Zuniga, A., Quillet, R., Perrin-Schmitt, F., and Zeller, R. (2002). Mouse Twist is required for fibroblast growth factor-mediated epithelial-mesenchymal signalling and cell survival during limb morphogenesis. Mech Dev *114*, 51-59.